Biomass and Bioenergy 184 (2024) 107201

Contents lists available at ScienceDirect

Biomass and Bioenergy

journal homepage: www.elsevier.com/locate/biombioe

Review article

Synthesis and applications of manganese oxide - biochar composites: A systematic review across catalysis, capacitor and sorption applications

Flora M. Brocza [a,*], Stella J. Foster [a], Caroline L. Peacock [b], Jenny M. Jones [a]

[a] School of Chemical and Process Engineering, University of Leeds, Leeds, LS2 9JT, West Yorkshire, UK
[b] School of Earth and Environment, University of Leeds, Leeds, LS2 9JT, West Yorkshire, UK

ARTICLE INFO

Keywords:
Biochar
Manganese oxide synthesis
Systematic literature review

ABSTRACT

Manganese oxide biochar composites (MnOx-BCs) are at the frontier of materials development for current environmental and engineering challenges in contaminant sorption and degradation, capacitive deionisation, as well as supercapacitor research. However, the parameter space for optimisation of such composites is vast, spanning from the choice of feedstocks and synthesis procedure to post-processing. This study uses a systematic literature review methodology to provide a comprehensive view into the synthesis methods and applications of MnOx-BCs. The focus is on the manganese phase oxidation states, which are often decisive for a material's properties but not directly comparable with the (well-explored) synthesis of pure MnOx due to the chemical variability of biochars. The relationships between synthesis method, manganese phase, crystallinity and morphology, as well as biochar type are characterised. We argue that careful selection of the desired manganese phase and oxidation state are as important as careful consideration of the bulk chemistry and microstructure of the biochar phase. Much evidence already exists for fine-tuning these combinations, but there is still a clear research gap in systematically studying the biochar impact on the final MnOx phase.

1. Introduction

Green carbon materials and their composites are at the frontier of materials development for current environmental and engineering challenges, with exponential growth in publications that detail their synthesis, characterisation and performance across a range of application domains. Manganese oxides (MnOx) possess a range of attractive qualities, such as their red-ox activity, electrochemical properties, large surface area, porosity, stability under a range of environmental conditions, low cost and environmental friendliness (e.g. [1,2]). Composites of green carbons such as biochars (BC) or activated biochars (ABC) and MnOx enjoy a particularly wide range of real-world applications due to the complimentary and sometimes synergistic properties of the two component phases As the studies in this review reveal, such composites show a great deal of potential; from material sciences to electrochemistry and environmental remediation (see Section 4). However, a gap in the structure-function relationships which underpin performance curtails the development and application of MnOx-(A)BC composites. This is because the parameter space for MnOx-BC composite synthesis and optimisation is vast. Both may be tuned for specific properties, e.g. oxidation state, surface area, or specific surface functionality, and nanomorphology; finally, the method of composite formation adds another dimension. To appreciate and understand the recent development on MnOx-BCs, it is vital to look beyond research disciplines and to explore how MnOx-BC composites are synthesised, optimised and applied in a variety of research contexts. Even though systematic reviews are less common in engineering, materials and environmental sciences than they are in e.g. the medical sciences, primary evidence synthesis can be crucial for understanding and applying the full potential of MnOx-BC composites. This publication is the first systematic, cross-disciplinary evidence synthesis on manganese oxide biochar composites, aiming to draw from all existing research to update the current understanding of the relationship between synthesis and function of manganese oxide — green carbon composites, while highlighting the properties necessary for successful application in a variety of fields.

After introducing MnOx, biochars and their desired characteristics in sorption, catalysis and capacitor applications, these properties are discussed in relation to the metadata on synthesis methods, manganese oxides and biochars collected from the reviewed studies. Finally, recommendations on synthesis methods and feedstock choice are given and research gaps are identified. The review is complemented by

Abbreviations: AC, Activated carbon; ABC, Activated biochar; BC, Biochar; BET, Brunauer-Emmett-Teller analysis; CDI, Capacitive desalination; MnOx-BC, Manganese oxide biochar composite

* Corresponding author.
E-mail address: pmfmb@leeds.ac.uk (F.M. Brocza).

https://doi.org/10.1016/j.biombioe.2024.107201
Received 6 March 2023; Received in revised form 29 February 2024; Accepted 25 March 2024
Available online 3 April 2024

a full data table of all reviewed publications in the supplement. It provides a reference and starting point for anyone wishing to synthesise MnOx(A)BC with properties that are tuned for the desired application.

1.1. Green carbon - Biochar

1.1.1. Defining 'biochar'

The term "biochar" has only appeared in scientific literature since the mid-2000s and has been applied in a variety of contexts. Following the definition of the European Biochar Certificate Foundation, biochar (BC) is a "heterogeneous substance rich in aromatic carbon and minerals", derived from biomass or waste materials by pyrolysis between 350 °C to 1000 °C in environments with low or no oxygen present [3]. Although also sometimes termed biochar, the products of torrefaction and hydrothermal carbonisation are excluded by this definition and also excluded from this review.

Activated carbon (AC) is generally produced at the same conditions, but the term is applied for carbons of any feedstock, including a fossil one such as coal, lignite, peat or fossil-based wastes (e.g. tyres, plastics). These feedstocks then undergo chemical and/or physical activation. While biochars were originally applied as soil ameliorators, they have since been optimised and refined into many different products, some of which include activation procedures, thus blurring the line between activated carbons and biochars ([4]). The definition of biochar in this review focuses on those pyrolysed carbons whose feedstocks are biogenic, but including materials which have also undergone an activation procedure.

1.1.2. Nomenclature for manganese oxide — green carbon composites

The following nomenclature is adopted for the rest of this text: **BC**denotes biochar , as defined in the above section and **ABC** stands for activated biochar. **(A)BC** is used to denote all biochars, raw and activated. Although not included in the systematic literature review, **AC** is used when discussing fossil-derived activated carbons. **MnOx** denotes any manganese oxide and is used as an umbrella term when the Mn phase or valence are not specified. It follows that **MnOx-(A)BC** is the umbrella term for all composites included in this study. Where it is necessary for the discussion, a specific material subgroup is addressed by specifying either the MnOx or (A)BC phase, e.g. β-MnO_2-ABC would be a composite of pyrolysite and activated biochar, $Mn^{3+,4+}$Ox-BC a MnOx with manganese (III,IV) valence or FeMnOx-ABC an ABC composite with both Fe and Mn oxides.

1.1.3. Properties of (activated) biochar

Porous carbon materials such as biochars and activated carbons are versatile and valued for their large and tunable surface area, pore structure, cation exchange capacity and electrical properties. Biomass itself can vary in its composition. Woody biomass, a common feedstock, is a lignocellulosic material made from the three main biopolymers — cellulose, hemicellulose and lignin, as well as organic extractives and inorganic minerals, in varying percentages and composition [5]. Different pyrolysis regimes are optimised for yields and different types of biochar. "Slow pyrolysis", characterised by a low heating rate and residence times from minutes to days, is preferred to maximise yield [6]. Fig. 1 gives an overview of how some material characteristics are influenced with pyrolysis temperature. Compared to the raw feedstocks, biochars exhibit a higher porosity and larger surface areas. The highest reaction temperature (HRT) is the most important factor which determines the reaction mechanism during thermochemical conversion of biomass [7]. The exact composition of a biochar depends on the feedstock, pyrolysis parameters and additives used in the process (e.g. [7,8]).

As a general rule, charcoals including biochars have negatively charged surfaces, producing basic pH values which increase with pyrolysis temperatures. The cation exchange capacity (CEC) of most biochars is dependent on the biomass feedstock and has been reported to be between 4.5–40 cmol g^{-1} [14]. Surface functional groups have been studied in great detail using a wide array of methods, such as Fourier transform infrared spectroscopy (FT-IR) [15], X-ray photoelectron spectroscopy (XPS) [16], Pyrolysis GC–MS [17], nuclear magnetic resonance (NMR) [18], Raman spectroscopy and NEXAFS [19]. Recently, electrochemical studies have established that apart from oxygenated surface functional groups or traces of transition metal phases involving Mn or Fe, the electrical conductivity of biochars may also be reason for its catalytic activity, involving redox-active *"quinone-hydroquinone moieties and/or conjugated π-electron systems associated with condensed aromatic (sub-) structures of the char"* [20]. Quinones have been directly identified on biochar surfaces by K-edge NEXAFS [19] and also using electron paramagnetic resonance spectroscopy, which has identified semiquinone-type radicals [21]. From this work, quinone/hydroquinone pairs have also been recognised as important electron accepting and donating entities in other types of carbonaceous matter, such as activated carbons and dissolved organic matter. Other carbonaceous materials such as graphite, carbon nanotubes, fullerenes and graphene oxides are also intensively researched for their electrochemical properties, both electrical conductance and electron transfer with other materials; these properties are attributed to their condensed aromatic structures with conjugated π-electron systems, which allow electrons to pass through the material. While sp2 hybridised orbitals in carbons increase with higher pyrolysis temperatures due to a higher proportion of the total carbon being in aromatic ring structures, quinones, which contain oxygen, decrease at high pyrolysis temperatures, thus, experiments on different pyrolysis temperatures have consistently shown that the electron donating and accepting abilities of biochars are highest at maximum pyrolysis temperatures of 400–500 °C [20]. It should however be noted that Prévoteau et al. [22] estimate total electron accepting and donating capacities to be significantly higher than in previous studies, up to 7 mmol(e-) · g_{char}^{-1} for a HRT of 400 °C, presumably due to slow kinetics which were not accounted for in earlier studies.

1.2. Manganese oxides

Manganese is a group 7 transition metal with an average atomic mass of 54.94 g/mol and 7 common oxidation states (7, 6, 4, 3, 2, 0, −1). Its oxides are ubiquitous in the environment. Composed of manganese in varying oxidation states and oxygen, they range from the rutile-structured MnO_2 and its polymorphs, to haussmanite $Mn_3^{2,3+}O_4$, $Mn_2^{3+}O_3$ and hydroxides, through to complex, layered or tunnel-structured $Mn^{3+,4+}$ minerals like todorokite and birnessite [23]. Table 1 gives an overview of the many naturally occurring manganese oxides (MnOx). For industrial applications, the ease of synthesis of MnOx with high purity, large surface area, varying degrees of crystallinity and tunable crystal nanomorphology [24], as well as variety of oxidation states and high electrochemical activity make MnOx a versatile class of materials. Additionally, MnOx are frequently less toxic to the environment than materials used in comparable applications (e.g. V_2O_5 in catalysts) and it is an abundant resource [23]. Accordingly, the synthesis of MnOx has been studied extensively in well-controlled settings (e.g. [24,25]), with outcomes in mineralogy and nanostructure influenced by the concentration and ratio of Mn ions of different oxidation states, redox conditions and pH and pressure conditions.

1.3. Applications of MnOx-(A)BC

Manganese oxide — biochar composites find widespread research interest in three distinct applications, based on different basic properties: capacitance, catalytic activity and sorption capacity. The specific MnOx-(A)BC applications as well as their targeted material properties are presented and discussed in depth in Section 4 . Clearly, the nature of MnOx delivered by the MnOx-BC preparation method is pivotal in its sorption/catalytic or supercapacity ability. This systematic review explores the tuning possible through synthesis route choices.

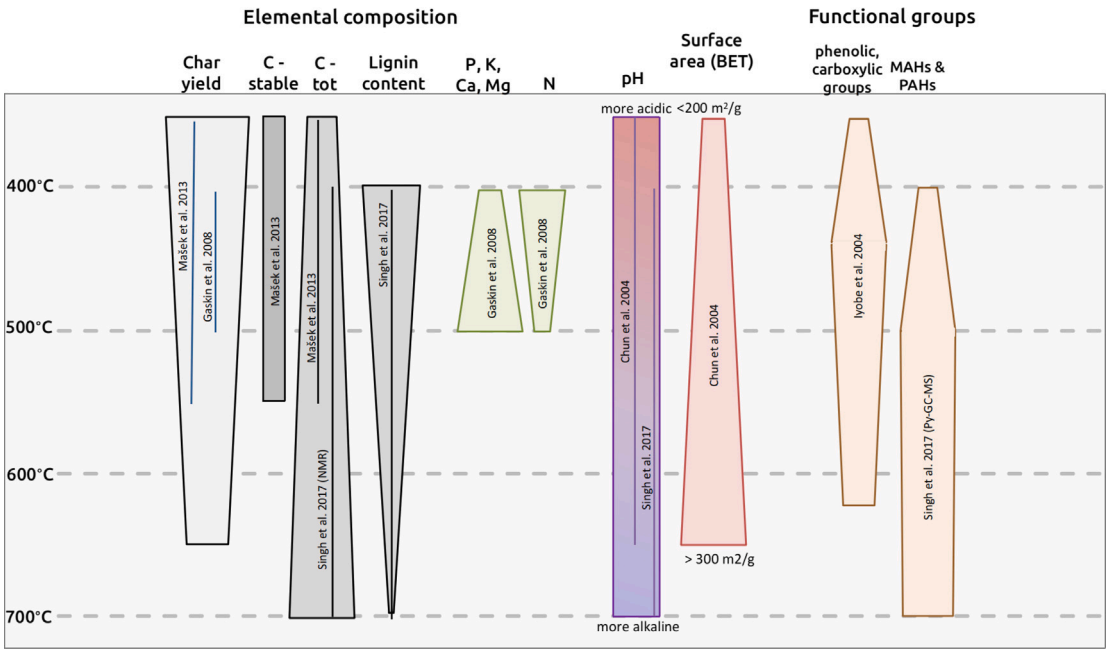

Fig. 1. Biochar properties with synthesis temperature.
Source: Data sources: [9–13].

Table 1
Important Mn oxide minerals and examples of their occurrence and applications.
Source: [23].

Mineral	Other name	Formula	Occurrence, use
1. Tunnel structured Mn oxides			
a. Manganese(IV) dioxides			
Pyrolusite	β-MnO_2	MnO_2	Abundant, f.ex. low-temp hydrothermal deposits.
Ramsdellite		MnO_2	Used in cry-cell batteries. Micro- and nano-
Nsutite	γ-MnO_2	$Mn(O,OH)_2$	structure controlled during synthesis [24,26,27].
b. Hollandite group $R_{.8-1.5}(Mn^{IV},Mn^{III})_8O_{16}$			
Hollandite		$Ba_x(Mn^{IV},Mn^{III})_8O_{16}$	Usually intermixed, low crystallinity; ores, solid ionic solutions, dissolved radioactive waste immobilisation, molecular sieves [28].
Cryptomellane		$K_x(Mn^{IV},Mn^{III})_8O_{16}$	
Manjiroite		$Na_x(Mn^{IV},Mn^{III})_8O_{16}$	
Coronadite		$Pb_x(Mn^{IV},Mn^{III})_8O_{16}$	
Romanechite		$Ba_{0.66}(Mn^{IV},Mn^{III})_5O_{10}$ * 1.34 H_2O	Formerly "psilomelane"; intergrowth with hollandite group in Mn ore deposits.
Todorokite		$(Ca,Na,K)_x$ $(Mn^{IV},Mn^{III})_6O_{12}$ * 3.5 H_2O	Common in soils and oceanic Mn nodules; mined for metals in interlayer.
c. Manganese hydroxides			
Manganite	γ-MnOOH	MnOOH	Like β-MnO_2, but O → OH, Mn^{4+} → Mn^{3+}.
Groutite	α-MnOOH	MnOOH	
Feitknechtite	β-MnOOH	MnOOH	
Pyrochroite		$Mn(OH)_2$	
2. Layered Mn oxides			
Lithiophorite		$LiAl_2(Mn^{IV}_2Mn^{III})$ $O_6(OH)_6$	$(Li,Al)OH_6$ interlayers.
Chalcophanite		$ZnMn_3O_7$ * 3 H_2O	Zn interlayers.
Birnessite group	"δ-MnO_2"	$[Na,Ca,Mn^{II}]Mn_7O_{14}$ * 2.8 H_2O	Interlayer cations not crystalline, may exchange; common in soils; use as sorbent for other HM. Large CEC.
Vernadite		MnO_2 * n H_2O	
4. Other oxides			
Hausmannite		$Mn^{II}Mn^{III}_2O_4$	Rare in nature; promising nanocatalysis nanomaterials [29].
Bixbyite		Mn_2O_3	
Manganosite		MnO	

HM : Heavy metals.
CEC : Cation exchange capacity.

Table 2
Inclusion and exclusion criteria applied to the screening and selection of studies.

	Inclusion criteria	Exclusion criteria
a	Full-length scientific publication with DOI	Conference proceedings, review articles, no DOI
b	Publication written in English OR abstract written in English, containing all relevant information for (b)	English full-text of the publication is not available; if an English abstract for a different-language is available, it does not contain the information relevant for inclusion.
c	The biochar/activated carbon materials can be identified as biomass-based from the abstract and title	The biochar/activated carbon materials are not biomass-based (i.e. made from car tyres, coal, plastics) OR the feedstock of the biochar/activated carbon is not specified
d	The publication describes a composite material between biochar/AC. The synthesis method is described in the methodology.	The publication describes any other interaction between biochar/AC and manganese (i.e. Mn sorption from wastewater) OR the entry does not clearly describe an interaction between Mn and Biochar/AC (i.e. Mn is only listed as a trace element within the biochar composition)

2. Systematic review methodology

The present systematic literature review was conducted according to the Preferred Reporting Items for Systematic Reviews and Meta-Analyses (PRISMA) guidelines [30].

2.1. Search strategy and eligibility criteria

This review builds on SCOPUS database entries between 1970 and November 24, 2022. Only original research entries with an available English abstract and DOI were considered. Where the publication body was not available in English, they were rejected if the abstract did not contain sufficient information for further classification, but were included if the aim of the paper included production of MnOx-BC and if method of material synthesis was indicated. Conference abstracts and reviews were not included. The search keywords used were "Manganese AND 'activated carbon' " and "Manganese AND biochar" with the search conducted on title, abstract and keywords of the publications indexed in the Scopus©Database. Activated Carbon was added to the search terms as it is often bio-based and there are significant inconsistencies in the usage of both terms (see Section 1.1.1). The entries found for "activated carbon" (AC) were then assessed based on whether there was an indication in the abstract of the paper, identifying the AC as bio-based or not by following the definition of Hagemann et al. [4]. Papers were rejected if they included activated carbon of unclear origin, or commercial activated carbon which could not be attributed to a feedstock. Only protocols producing manganese oxides or mixed oxides were considered; other Mn compounds such as phosphates or sulphides were not included in the search. The full list of inclusion/exclusion criteria are listed in Table 2 and the screening procedure according to PRISMA guidelines is given by the scheme in Fig. 3. After pre-screening, only entries fitting the above eligibility criteria were retained in the record list. Of these, entries were divided into four categories based on the information presented in the abstract, depending on the predominant application types for MnOx-BC materials: "Remediation through sorption", "catalysis", "capacitors", and "other". The methods sections of all recorded papers were then read and information was tabulated as outlined in Table 3. Information on analytical techniques and MnOx phase/morphology were also collected where available. Upon closer reading, a total of 432 different synthesis protocols were retrieved from the included publications.

2.2. Appraisal of information quality

Most of the collected information for this review (e.g. biochar feedstock, synthesis method and procedure, intended application) did not require additional quality assurance. The suitability of a MnOx-(A)BC composite for the specified application was clearly indicated in the studies through experimental data, which were also collected in the database and can be compared against each other, taking into account the specific experimental conditions. This information was tabulated, but does not present the main body of this review, which focuses on preparation procedures. However, as MnOx are often poorly crystalline, it can be difficult to determine the exact mineralogy and manganese oxidation states of a phase using only X-ray diffraction or energy dispersive spectrometry on a scanning electron microscope. Where this information was collected from individual studies, the combination of analysis techniques which led to the result were recorded as well, to ensure a solid base for the identification.

3. Discussion: MnOx-(A)BC synthesis

The results are grouped into key insights pertaining to the role of the biochar phase in the literature sample and particularly the relationship between synthesis method and MnOx phase, and application-specific observations.

3.1. The biochar phase: Feedstocks, activation procedure and pyrolysis

> **Key Insight 1:** Biochar feedstocks are presented as sustainable, cheap and versatile in most of the papers utilising them. Few studies compare different biochar feedstocks or justify the use of one particular biomass feedstock over another, showing large potential in exploring and fine-tuning the precursor choice, the pyrolysis temperatures, specific pore structures, surface functionalities and/or activation procedures of biochars.

The biochar feedstocks of the reviewed literature represent a great variety of biomass and waste materials, from agricultural residues generated in large quantities, to manure, sewage sludge, and wastes from brewing or production of medicinal herbs. On top of this diversity, the choice of pyrolysis temperatures adds variability in material properties, and different activation procedures were applied to the subset of activated biochars (denominated ABC), ranging from physical activation with steam or CO_2, to chemical activation using $KMnO_4$ (e.g. [31]), KOH or acids as activation agents. Depending on the designated application of an (A)BC-MnOx, either activated ABC or 'raw' BC dominate the reviewed literature: while in catalysis applications, over 87% of publications used ABC, oer 70% of sorbent publications relied on unmodified BC. The frequency of use of different activation agents is given Table 4.

It becomes clear that apart from the common 'operational' definition of biochars, it is challenging to interpret how different biochars would react during synthesis, or even to extract predictive synthesis-function relationships of this dataset. It is notable how few explicitly mentioned properties of their biochar or even feedstock biomass in the discussion, beyond observations of BET surface area and bulk chemistry. While capacitor literature frequently included detailed descriptions of the biochar phase nanomorphology (e.g. [32,33]) as a crucial factor for the efficacy of the supercapacitor, other papers only refer to mixtures of biochar feedstocks like 'agro-waste' without further characterisation before pyrolysis (e.g. [34]). This reflects that the price point, availability and low environmental impact of a feedstock are often key considerations for the use of a certain material, rather than unique suitability to the studied application. Where different feedstocks, pyrolysis conditions and/or activation procedures were compared, a difference in performance could be found:

Table 3
Details on the full-text data collection from included references.

Title, abstract, author list	
Paper identifiers	Author, year, DOI
Type of biogenic carbonaceous material	*N* - not biogenic, not carbonaceous ⟶ rejection; Y - biogenic, carbonaceous ⟶ inclusion; Biomass: raw, non-pyrolysed biomass; specify biomass; Char: specify biomass; AC: Activated carbon; specify biomass and activation agent; Other bio-based carbonaceous materials: graphene, nanotubes, nanowires, nanofibres
Materials and methods	
Synthesis protocol	Mn reagents used for synthesis; In case of mixed oxides: which other dopant/metal salt was used?; Reaction conditions (Acidic? Basic? Organic solvent(s)? Autoclave? Temperature? Stirring/Sonication?)
Heat treatment	N; Y- Oxic/anoxic? How long?
Final washing/drying	Washed with water? A solvent?
Analytical techniques applied	XRD, BET, XPS, SEM, TEM, Raman spectroscopy, FT-IR, others
Introduction, Results, Discussion	
Mn oxide phase	MnOx, Mn-Fe oxide, Mn-Ce oxide, etc.
Mn oxidation state(s)	"Mn^{4+}", "Mn^{4+}, Mn^{3+}", "Mn^{3+}", "Mn^{3+}, Mn^{2+}", "mixed", "unknown"
Application area and details	Sorption: Aqueous or gaseous application? Target sorbent? Catalysis: Low temperature catalysis? Which reaction is catalysed? Capacitors: Supercapacitors or capacitative deionisation?
Any mention of 'competing' materials for this particular application?	Free text, only selected publications
Which factors are listed to identify the MnOx-BC as a success/failure?	Free text, only selected publications

1. Different pyrolysis and activation procedures on the same material. Whether optimising the pore structure, surface functionality or other properties of a biochar, pyrolysis and activation procedures have a large influence on the final product. Of the surveyed publications, 45% opted for physical or chemical activation, while 55% used 'raw' biochar for further MnOx impregnation, the remaining using different or unspecified protocols. Systematic comparison between pyrolysis and activation procedures of the (A)BC phase were much fewer, but shed light on the large differences in functionality of the materials.

Pyrolysis temperatures: Chacón et al. [35] compared $KMnO_4$ activation on olive branch biochar at 400 °C and 1000 °C, which had a clear influence on the results of soil remediation incubation experiments for this char. Under aerobic conditions, BC-1000 °C showed the best degradation performance for pentachlorophenol, while the oxidised BC-400 °C performed well under both aerobic and anaerobic conditions and showed the highest redox capacity. The extent of remediation was found to depend on redox capacity, but the rate of the reaction was determined by the material's conductivity. Similarly, Qiu et al. [36] systematically tested the impact of not only pyrolysis temperatures (400–800 °C) but also residence times at maximum temperature (0.5–4 h) on their sewage sludge-derived biochar sample set. They found that ideal biochar porosity was reached at 700 °C for their studied process, persulfate activation to degrade an anthraquinone dye. It may also be desirable for a MnOx-BC to withstand higher temperatures. For example, Li et al. [37] could regenerate their sewage sludge MnOx-BC at 450 °C, desorbing the collected antibiotics from it, as the material was originally pyrolysed at 1100 °C, thus proving the material's recyclability for antibiotics remediation from waste water.

Activation procedures: Maneechakr and Karnjanakom [38] compared four different activation procedures on palm kernel cake biochar carbonised at 350 °C: one physical, three chemical with (I) HNO_3, (II) $KMnO_4$, (III) HNO_3 + $KMnO_4$. The materials were tested for application in Fe, Ca and Zn sorption and protocol (II) yielded consistently the highest sorption capacities for all cations, in the order of $Fe^{2+} > Fe^{3+} > Zn^{2+} > Ca^{2+}$, attributed by the authors to synergistic effects between the carboxylic groups and surface MnO_2. An example of comparison of two physical activations, Yang et al. [39] prepared steam activated and CO_2 activated walnut shell biochar, which was then mixed with different commercial pyrolusite samples to make up β-MnO_2-ABC and found the H_2O-activated sample to show higher and more prolonged activity in selective catalytic reduction due to a larger BET surface area and more oxygenated functional groups. Similarly, Liao et al. [40] also saw differences in properties between pig manure BC and pig manure AC modified by H_2O_2, $KMnO_4$ for U(VI) sorption. Clearly, activation is an important factor for the properties and performance of the biochar in all papers where such comparisons exist. There are not sufficient systematic studies to draw firm conclusions around which procedures are best and indeed, it might depend not only on the biochar precursor, but also on the intended application of the material which poses a multi-faceted optimisation challenge to every researcher and engineer.

Systematic optimisation: Yu et al. [41] present a true optimisation procedure, following a Taguchi orthogonal experimental design procedure for screening the best-suited biochar feedstocks, pyrolysis temperatures, activation agents and manganese loading of their material [41]. Their detailed observations reveal nitric acid treated ABC to deliver favourable pore structure for manganese impregnation and 800 °C to be the optimal pyrolysis temperature for low-temperature deNOx of flue gas. Liu et al. [42] present a different approach, systematically optimising not only activator concentration, but solid–liquid ratio, calcination temperature, calcination time and sludge to Fe_2O_3-MnO_2 ratio on their sewage sludge-derived BC. A further positive example includes Lee and Shin [43], who compared different activation procedures (alkaline, acidic, 'oxidic', KMnO4, FeOx) and three different biochars (rice husk, wood chip, a commercial composite material) at a constant pyrolysis temperature.

2. Different feedstocks on the same synthesis procedure. As opposed to comparing activation procedures, Yu et al. [41] conducted optimisation of their material on rice husk, corn cob and lotus leaf biochars, finding that lotus leaf biochar consistently outperformed the other two feedstocks at equal pyrolysis conditions, activation procedures and manganese loading for selective catalytic reduction of NOx by NH_3. They cite good resistance to H_2O, suitable surface acidity and a higher redox capacity as reasons for the good performance. Similarly, Lalhmunsiama et al. [44] produced ABC and MnOx-ABC from areca nuts and rice husks. The rice husk MnOx-ABC contained more manganese by weight percent and showed the highest Cu^{2+} and Pb^{2+} removal under a variety of conditions, which was attributed to a difference

in pH_{PZC} of the samples. Pierri et al. [45] also compared different agricultural residues in their performance as Mn^{2+} alkene epoxidation catalysts, finding that chars with a higher degree of graphitisation exhibited faster reaction kinetics, but that there was a trade-off with material stability and reusability. A larger sample matrix was compiled by [46], who compared nine different BCs produced at the same pyrolysis temperature and the final jacobsite $MnFe_2O_4$-BC were tested for Cu(II) sorption. The feedstocks included fibres, fruit shells, bamboo, pinecone, and agricultural residues. They did not find correlations between surface area and functional groups with aqueous Cu(II) sorption, concluding that the jacobsite surface impregnation, rather than BC-inherent characteristics, determined successful sorption.

3. Variable amount of manganese on the char surface. Several studies report that the MnOx impregnation procedure had a negative effect on BET porosity (e.g. [47]). Jia et al. [48] systematically evaluated the effect of Mn loading of a Fe-MnOx-BC and a Fe-$KMnO_4$-BC on BET surface area; while the original walnut shell biochar had a low BET surface area of 39.21 $m^2\ g^{-1}$, surface area generally increased with Fe-Mn impregnation, but reached a maximum of 288.76 $m^2\ g^{-1}$ with 2% Mn impregnation, which then decreased to 251.14 $m^2\ g^{-1}$ at a Mn loading of 6%. The Fe-$KMnO_4$-BC char also increased BET surface area, but by less; at 2% $KMnO_4$ loading, it reached a maximum value at 158.45 $m^2\ g^{-1}$ and then decreased to 78.01 $m^2\ g^{-1}$ at 6% $KMnO_4$ loading. Similarly, Faheem et al. [49]describe an increase in BET surface area from 234.8 $m^2\ g^{-1}$ of rice husk biochar to 430.2 $m^2\ g^{-1}$ on a biochar with 2.26 wt% Mn content after a $KMnO_4$ impregnation procedure, but a further decrease in materials with 6.58 wt% Mn loading (BET = 340.0 $m^2\ g^{-1}$) and 6.96 wt% Mn (BET = 260.0 $m^2\ g^{-1}$), also reporting pore size decreases from 3.34 in the blank biochar to 2.18 nm at the highest Mn loading (6.96 wt%). Wang et al. [50] tested pine wood BC pyrolysed at 700 °C, impregnated with 0.9, 3.7 and 10.0 weight % Mn content and concluded that 3.7% was optimal for Pb^{2+} sorption as 10% Mn loading led to pore clogging. Kamran and Park [51] explore MnO_2-BC of rice husk and coconut shell – two of the most frequently studied BCs – for lithium sorption, finding that variation in the amount of $KMnO_4$ used in wet impregnation was the main predictor of high Li sorption capacity, rather than differences in the feedstocks. In conclusion, it appears that MnOx impregnation procedures lead to an initial increase in surface area due to the high surface area of amorphous MnOx materials. However, surface area reaches a maximum and decreases with further loading, possibly due to surface pore clogging on the BC.

3.2. Interplay between synthesis procedure and MnOx mineralogy

Key Insight 2: The biochar feedstock is a significant part of the reaction, and there is evidence that it influences the Mn mineralogy outcome. Systematic studies and experimental design for a specific application for different feedstocks, pyrolysis conditions and Mn loading are essential for optimal feedstock choice.

Key Insight 3: The choice of synthesis protocol has a strong bearing on the manganese oxidation states, mineralogy, surface area and nanomorphology of the resulting MnOx-(A)BC, in turn influencing performance. It should be chosen with careful consideration of literature across research disciplines and across the full MnOx-(A)BC application range. Special attention should also be paid to heat treatment of freshly synthesised MnOx-(A)BCs, which can optimise crystallite size, but also lower Mn oxidation states.

3.2.1. Manganese sources

Most papers rely on the chemical reagents $KMnO_4$, $MnCl_2$, $MnCO_3$, $MnNO_3$, $MnSO_4$ and $Mn(CH_3CO_2)_2$ for MnOx synthesis. Some studies also utilise spent batteries [52–54] and pyrolusite mineral powder [39,55–58] as their Mn feedstock, which is notable from a sustainability perspective. In some cases where sewage sludge was the biochar feedstock, Mn was already present in sufficient [59,60]. The use of manganese-hyperaccumulating plants like *Phytolacca americana* and *Sedum alfredii*, which were grown in heavily contaminated soil or irrigated with $MnCl_2$ solution under laboratory conditions, is also reported [61–63]. Of all synthesised MnOx-(A)BC in this review, 40% of the final products are not pure MnOx, but rather binary mixtures with another metal. This is especially common in sorption and catalysis applications. For example, more than a quarter (28%) of the protocols yield MnFeOx-BC composites, which are reported to combine the superior sorption capabilities of Mn oxide impregnated chars with the ease of handling of magnetic materials, which may be retrieved more easily from environmental settings (e.g. [64]). In catalyst applications (e.g. mercury oxidation) and sorption of As_6^{3+} [65], synergistic effects between Mn and Ce, another common metal pairing, are exploited. Mn is incorporated into the CeO_2 lattice, providing more active sites for catalytic reactions [66,67]. In addition to re-oxidising Mn^{3+} to Mn^{4+} after a reaction, Ce shows strong resistance to SO_2, which commonly poisons flue gas oxidation catalysts [68]. The impact of synthesis method on the average oxidation state of Mn in MnOx-(A)BC is shown in Fig. 5 and discussed in the following sections.

3.2.2. Findings by synthesis method

This section aims to provide the reader with a comprehensive overview of MnOx-(A)BC synthesis techniques, reporting how commonly they are used, and whether the resulting materials show some notable features to be considered when designing a MnOx-(A)BC for a specific application. This is illustrated by case studies, to be followed up by the reader.

Wet impregnation. Out of a total of 432 surveyed protocols, 60% are produced by wet impregnation procedures whereby a pre-made BC or AC is immersed in aqueous solution in which at least one type of manganese salt is dissolved. To better disperse the Mn on and in the biochar, several protocols use sonication or other forms of agitation at various intensities and lengths (e.g. [69,70]). Further variables are temperature, acidity and alkalinity of the solution. The application of several manganese components with different oxidation states (e.g. manganese(II) such as chloride or sulphate, followed by a second impregnation step of manganese(VII) in the form of $KMnO_4$) is required by many protocols. This variety is well reflected in [71], who produce four different polymorphs of manganese dioxide (α-MnO_2, γ-MnO_2, δ-MnO_2, ϵ-MnO_2) through various wet impregnation procedures, showing that high precision is possible with tight process control. Subsequently, the solutions are filtered, dried, and in many cases (44%) subjected to further heat treatment under oxic or anoxic conditions.

Hydrothermal method. The second-most common synthesis technique is hydrothermal treatment, where one or several manganese salts, alongside other metal salts and biochar, are autoclaved at temperatures between 60 and 200 °C for 1–24 h. In some cases (e.g. [72]), the product is subsequently pyrolysed in an N_2 atmosphere at 500 °C. In 40% of the cases, other metal salts are added. The majority of hydrothermal synthesis papers explicitly indicate that a specific nanomorphology was synthesised, echoing reviews of transition metal synthesis protocols like Qiao and Swihart [24] that a high level of process control is possible in hydrothermal systems. To achieve different crystal structures and morphologies, the hydrothermal reaction parameters are systematically tested (e.g. [27,73]). The intended use of these materials is usually for application in cathodes or batteries, or as catalysts [74]. The study sample did not include literature where the effect of biochar feedstock on the final MnOx nanomorphologies were reported, indicating a gap in the literature.

Deposition pre pyrolysis. Another synthesis option is the immersion of raw biomass in a solution containing a manganese salt before pyrolysis. In 34% of the cases, another metal salt, mostly $FeCl_3$, is added to produce Mn-Fe oxides. This type of synthesis procedure is prevalent in sorption literature and it is not possible to link it with a preferred manganese valence. While in most cases, the intention was to produce actual composites of MnOx and BC, this category also includes instances in the literature where the introduction of MnOx to the biochar surface is merely a byproduct of using $KMnO_4$ as the activation agent in the process of activated carbon production (e.g. [75]). Protocols pyrolysing naturally Mn-rich sewage sludge are also included here [59]. Wang et al. [76] compare pre-deposition MnOx-BC (using $MnCl_2$ as the Mn source) to a material produced by an acidic wet impregnation procedure modelled after a birnessite synthesis protocol [77]. They conclude that the more crystalline Mn^{II} Ox-BC, produced by pre-deposition, performed worse in the sorption of As^{5+} and Pb^{2+} than the $Mn^{III,IV}$ Ox-BC from wet impregnation with $KMnO_4$.

Sol–gel methods. Sol–gel processing generates monolithic solids from colloidal gel-like solutions. Cross-linking is induced in the colloidal phase to form long range structures within the solution, often with a low overall volume fraction. The resulting gel is then subject to one of several possible drying processes which leaves a low density and often highly porous solid structure. The drying parameters play a large part in determining the final porosity of the solid. Sol–gel processes are further divided up into aero-, xero-, and cryogels, as per the mode of drying used to remove the solvent from solution. Where hydrothermal techniques such as autoclaving are used, the materials are called hydrogels. The cross-linking molecules in this literature collection have varied widely, from liquefied wood char [78–80] to sugars like glucose and sucrose [34,81], to egg whites [82]. Alginate-biochar hydrogel beads are noteworthy as they do not rely on the introduction of a separate cross-linking agent to initiate gelation and instead present a self-contained structure for MnOx-BC [52,83]. The important drying step (e.g. vacuum drying [84]) as well as the need for crosslinking agents makes this synthesis route more involved and potentially expensive than some other techniques. These materials allow great process control, especially over the porosity of a material and also over the manganese phase, as evidenced in Fig. 5, where most studies report a well-defined Mn oxidation state, but further generalisation is not possible given the large variability in sol–gel processes applied. Many reported sol–gel MnOx-BC composites are applied for (photo)catalytic degradation of water pollutants [78–80] as well as contaminant immobilisation [82].

Physical mixing. Mixing of commercial MnO_2 powder or naturally occurring pyrolusite β-MnO_2 with varying amounts of Fe contents is another simple synthesis method. It can also be applied to construct an asymmetric capacitor. In some cases, the Mn^{4+} mineral phase and biochar were subjected to an oxygen-deprived calcination step, which can be assumed to lead to reduced Mn oxidation states. This accounts for the trend observed in Fig. 5. Liu et al. [55] report that the mineral-augmented pyrolysis had a positive effect on the presence of mesopores in the MnOx-BC, which resulted in more sorption of dye in an aqueous solution, compared to activated carbon without any mineral addition.

Deposition-precipitation, combustion synthesis and electrochemical deposition. Rather than wet impregnation, where the solid MnOx-BC is filtered after immersion in a Mn solution for a specified amount of time, deposition-precipitation synthesis works with a slurry with a higher solid-to-solution ratio. Instead of a filtering step, the slurry is subsequently evaporated to dryness in a furnace or water bath, similar to incipient wetness impregnation (e.g. [65,85]). In combustion synthesis, a wet slurry consisting of biochar precursor and Mn chemicals and others is heated in a furnace for a short amount of time [59,86,87]. Electrochemical deposition was applied in two cases of capacitor production, where the conductive activated carbon/biochar was used as the working electrode in a solution containing Mn acetate and Na_2SO_4. In a setup with counter electrode (e.g. platinum foil in the case of [33]) and reference electrode (e.g. Ag/AgCl [33]) a constant current was applied [88] and MnO_2 was deposited onto the biochar. After a set deposition time, the MnOx-BC was rinsed and dried. It is noteworthy that this method can only be applied to (activated) biochars with enough structural integrity to serve as an electrode, such as the activated carbon textile in the case of [33] and the pyrolysed wood platelets in [88]. While there are not enough datapoints for an analysis of preferred oxidation states in combustion synthesis and electrochemical deposition (see Fig. 5, 'Other'), deposition-precipitation synthesis on (A)BCs tends to produce mixed MnOx.

Other notable treatments. A number of other noteworthy synthesis methods include pen lithography, where MnO_2 are mixed into an ink [89]; or spray sorption, where manganese(II) is sprayed on the finished biochar, meant to be easily available to the surrounding soil as micronutrient-boosting soil amendment [90].

3.2.3. Heat treatment after impregnation

Additional heat treatment steps after the impregnation of ABC with manganese are frequently encountered in literature, either to increase crystallite size or to achieve a specific mineralogy. However, it is observed that the most common form of heat treatment, pyrolysis in an anoxic atmosphere, consistently leads to low manganese valences (Fig. 6). Examining the anoxic/low oxygen data further, 6 out of the 9 publications which specify Mn^{4+} oxide only used SEM and XRD to identify the mineral phase, or refer to other publications, leading to some uncertainty in the accuracy of this claim. This finding is relevant because heat treatment in air and under anoxic conditions (N_2, Ar) of manganese oxides is known to induce phase transformations and gradual morphological change to MnOx nanoparticles. Deljoo et al. [91] studied cryptomelane-type MnOx, noticing a transformation to cubic Mn_2O_3 around 500 °C and to Mn_3O_4 at around 1000 °C in air, as well as a transformation from spherical towards platelet-shaped nanomorphology. Heat treatments in Ar lead to the formation of Mn_3O_4, then Mn_2O_3 around 475 °C, then changing back to Mn_3O_4 at temperatures over 830 °C and further to MnO above 1000 °C. This indicates that, if applied intentionally, much fine-tuning can be conducted during the heating step. However, few of the publications included in this review seemed to display this degree of intentionality about the Mn oxide phase during transformation, making misinterpretations of their samples' manganese mineralogy and subsequent properties possible.

3.2.4. Synthesis procedure and Mn oxidation states

Fig. 5 gives an overview of the relationship between reported Mn oxidation states and synthesis protocol used in all studies where this information could be extracted. In wet impregnation, the resulting composites vary as widely as the synthesis procedures themselves, exhibiting a range of manganese mineral phases. However, not all publications report the Mn phase of the final product, often using the umbrella term "MnOx" and instead reporting the relevant performance indicators, such as sorption capacity for a specific heavy metal. A general tendency towards lower oxidation states (Mn^{2+}, Mn^{3+}) can be observed in wet impregnation protocols using Mn^{2+} salt precursors, as well as $KMn^{7+}O_4$ precursors that undergo oxygen-free or deprived heat treatment (pyrolysis), often under N_2 atmosphere. On the other hand, the majority of hydrothermal synthesis papers explicitly report that their composite contained Mn^{4+} as the final Mn phases. In deposition before pyrolysis, there is a tendency towards mixed-valence MnOx and lower Mn oxidation states as Mn phases under go a pyrolysis step, as discussed in Section 3.2.3. Across synthesis procedures, the use of $KMn^{7+}O_4$ in a synthesis protocol is a strong indication of a resulting MnOx of higher manganese valence, the median oxidation state of $KMnO_4$-impregnated samples being 4 (see Fig. 4).

4. Discussion: Applications

4.1. MnOx-ABC for (super)capacitors

4.1.1. Material properties of MnOx-BC (super)capacitors

Supercapacitors are materials whose capacitance is magnitudes higher than that of traditional capacitors (10-100x more energy per unit volume or mass than electrolytic capacitors). They operate on two principles: double layer capacitance and pseudocapacitance. [92] Double-layer capacitance occurs due to charge separation at the interface between the electrode and electrolyte. Carbonaceous materials such as activated carbon, graphene and carbon nanotubes are classically known to exhibit mainly this type of capacitance. Pseudocapacitance, on the other hand, happens through redox reactions in the electrodes. Transition metal oxides are typical electrodes for pseudocapacitors. Manganese dioxide is a strong contender for the positive electrode of asymmetric supercapacitors due to its high specific capacitance, wide potential range, low cost, low environmental impact and easy availability [93]. The main drawback of MnO_2 is its poor electrical conductivity of 10^{-5}-10^{-6} S cm^{-1} [94]. This is circumvented by synthesising a variety of nanostructures such as porous MnOx, thin films, needles or nanosheets through controlled synthesis [95,96]. MnOx-carbon composites are also attractive due to the carbon's favourable low electrical resistance, thermal stability, large specific surface area and porosity. Wu et al. [96] provide an up-to-date review on this matter. Another encountered application are MnOx-(A)BC for capacitive desalination (CDI): Here, the electrosorption capacity (in mg g^{-1}), surface area, ion storage and ion removal kinetics are additional decisive parameters for the success of the material [97–99].

> **Key Insight 4:** MnOx-(A)BC electrodes need highly controlled MnOx phases and biochar nanomorphology, so the choice of BC feedstock is highly relevant. Hydrothermal synthesis is preferred for good process control.

4.1.2. MnOx-(A)BC (super)capacitors in literature

Research on supercapacitors tends to focus on advanced carbon materials such as graphene and carbon nanotubes, as the nanomorphology of both MnOx and the carbon material are highly important for the performance of the composite. Generally, asymmetric supercapacitor designs are favoured in the reviewed literature, in many cases made up by a MnOx-BC (e.g. MnO_2/activated biochar) positive electrode and a pure activated biochar negative electrode (e.g. [33]). Other cases report a MnOx phase as positive electrode and pure activated biochar as the negative electrode (e.g. [86] or a NiO-MnO_2 nanoshell composite and pomelo peel/buckwheat hull biochar [100]).

Biochar phase. (A)BC-based supercapacitors tend to perform worse than materials such as graphenes and carbon nanotubes but activated carbons are the most common supercapacitor materials due to a better price and larger available quantities. A review including literature up to August 2019 found that roughly 14% of primary research on MnO_2-carbon supercapacitor materials was conducted on activated carbons, with the other 86% focusing on composites with graphene, carbon nanotubes and carbon nanofibres [96]. However, the chemical, and structural diversity of bio-based activated carbons and biochars can also work to their advantage. In several instances, literature in this review showed that the macrostructure of the original biomass has benefit for the biochar morphology, as in [32] where human hair was used to achieve 2D nanosheet morphology on the biochar and needle morphologies in the MnO_2 which was well-distributed on the composite surface. Wei et al. [101] used porous lotus seed pods for hollow structures. Comparisons between different biochars reveal significant differences in their performance (Table 5). An example is the comparison of buckwheat hull, pomelo peal and activated carbon as asymmetric capacitors, finding that buckwheat hall MnOx-ABC delivered the best cycling stability [100]. The literature shows that intricate morphologies such as MnO_2-nanoflowers [33] and needles [32] can also be achieved with bio-based feedstocks. In the case of [32], the original morphology of the feedstock – human hair – was exploited for this result.

MnOx phase. Where specified, highest specific capacitances and electrosorption capacities are produced by hollandite α-MnO_2 (e.g. [88,98,99,102]) produced by wet impregnation, hydrothermal and electrochemical deposition methods — the latter being exclusively used in capacitor experiments. Half of the protocols utilise hydrothermal setups, which allow close process control and are suitable to create the needle or nanoflower structures which are needed to compensate for the low electrical conductivity of MnOx.

4.2. MnOx-ABC for catalysis applications

4.2.1. Material properties of MnOx-BC catalysts

Manganese oxides, being a diverse and tunable class of semiconductor species, have a large potential for application in heterogeneous catalysis. Likewise, MnOx-BC composites are frequently studied for oxidation (photo)-catalysis. It can be generalised that MnOx are the catalytically active component, while biochar is mostly seen as the support. However, there is ambiguity surrounding the properties (e.g. band gap) of specific bulk MnOx for specific (photo)oxidation reactions [103]. Good carbon-based catalyst supports provide appropriate mechanical strength, may act as a heat sink or source, and act to optimise the dispersion of the active component and the bulk material density. They may deliver optimised surface area, pore size and crystallinity of a material, while also adding to the chemistry of the catalyst, for example an increase in its activity, or minimising negative effects such as sintering and poisoning [104]. The requirements for the manganese phase of the composite differ strongly depending on the type of reaction to be catalysed, and has already been reviewed elsewhere: Ristig et al. [103] review MnOx in heterogeneous (photo)catalysis; Carney et al. [105] summarised reactions of manganese catalysts in chemical synthesis and [28] do the same for cryptomelane molecular sieves; Jia et al. [106] review manganese(III) (oxyhydr)oxides in advanced oxidation processes, revealing significant differences in catalytic properties even within $Mn^{III}Ox$ phases. The detailed interplay between crystal structure, band gap, Mn valence, nanomorphology, degree crystallinity and bonding sites on the MnOx surfaces can only be discussed in relation to the specific target reaction to be catalysed, and ambiguity still exists around the properties of the MnOx phases, as they often occur in mixed phases. Zhang et al. [107] review the application of MnOx catalysts as flue gas NOx reduction catalysts. In this setting, $Mn^{IV}O_2$ and $Mn_2^{III}O_3$ were identified has having the highest activity and N_2 selectivity.

4.2.2. Catalytic degradation in aqueous systems

> **Key Insight 5:** Catalytic degradation of contaminants in aqueous solutions makes use of the (photo)catalytic activity and dynamic redox potential of MnOx-(A)BCs. While organic carbon moieties are also known as natural (photo)catalysts, (A)BCs are utilised as catalyst supports and possibly sorbents in this context. The stability and activity over a large pH range, as well as large surface area and microporosity are beneficial in a large range of contexts but the optimal MnOx-(A)BC depends on the catalysed reaction.

Catalytic degradation of synthetic dyes, antibiotics and other organic molecules is a broad field of application for MnOx-(A)BCs. While photodegradation and heterogeneous Fenton-like degradation rely on the production of free radicals to target and break the bonds of organic molecules, others rely on oxidation–reduction mechanisms for destruction of their target. Heterogeneous Fenton-like processes are also advanced oxidation processes which generate non-selective oxygen species such as hydroxyl radicals in situ. Photo-Fenton reactions can

be used to degrade organics at a wider pH range than heterogeneous Fenton-like reactions. Advanced Oxidation Processes (AOP) may be catalysed by a range of carbons, as well as manganese and its oxides (e.g. [108]). Catalytic ozonation processes induce ozone decomposition and hydroxyl radical formation via a variety of pathways, using transition metal ions as catalysts.

In natural waters, dissolved organic matter and transition metals are the most common photocatalysts for radical generation, so MnOx-BC composites are promising materials for this application which may both mimic and enhance natural processes with little disturbance to the system [109]. Several publications focus on the photodegradation of aquatic contaminants such as synthetic dyes or antibiotics (e.g. [78,110,111]). Successful MnOx-BC exhibit a high photocatalytic activity under visible light conditions, high photochemical stability and are durable over long periods of repeated use. Heterogeneous Fenton-like processes were employed e.g. to degrade tetracycline and PAHs/naphthalene [110,111]. Especially noted was the ability to exploit this reaction mechanism with MnOx-(A)BC to be applied to a wide pH operating range. Nawrocki and Kasprzyk-Hordern [108] provide a review of different ozonation pathways in the context of aqueous pollutant degradation, and review a number of publications studying dissolved Mn ions in homogeneous catalysis, as well as MnOx in heterogeneous catalytic ozonation, stating that MnO_2 is the most widely studied manganese phase for this purpose. Wu et al. [47] produced an activated carbon-MnOx composite from yeast feedstock that outperformed pure yeast AC in the total organic carbon (TOC) removal efficiency, but exhibited larger phenol uptake and a smaller BET surface area. Oxalic acid was degraded by heterogeneous catalytic ozonation using a MnOx-activated sewage sludge composite with different Mn loadings were studied by [112] and they concluded that the reaction was only feasible at low pH (optimum at pH 3.5). Other catalytic applications include peroxydisulfate-AOP of chlorinated organic pollutants using magnetic α-MnO_2-Fe-BC [113] or sulphate radical-based advanced oxidation processes where MnFeOx-BC is used to activate peroxymonosulfate to produce $^{\cdot}SO_4^-$ radicals [64,114]. The long half life and good performance in a large pH range (pH 2–8) are noted. Zhou et al. [113] also note that graphitic biochars are favourable catalyst supports in this application. MnO_2 is, among suspended particles of the other semiconductor oxides (e.g. ZnO, Fe_2O_3 and TiO_2), the most important photocatalyst in natural waters [109] and routinely synthesised. However, the surveyed catalyst literature had the largest proportion (30% of publications) where the manganese oxdiation state and phase were unknown. Where specified, mixed manganese(II,III) oxides, often binary oxides like jacobsite $MnFe_2O_4$ and $LaMnO_3$ synthesised with iron or lanthanum showed good results for photodegradation of different pollutants, with FeMnOx being valued for the possibility of magnetic separation after usage in aqueous systems. One publication mentioned that the co-existence of manganese(III) and (IV) is favourable for photocatalytic degradation of synthetic dyes [84]. Mn^{4+}Ox-BC with controlled nanomorphology showed promising results for BPA degradation (δ-, α-MnO_2), but was reported as underperforming as the electrocatalytic support in a microbial fuel cell (β-MnO_2). Sol–gel and wet impregnation syntheses were commonly used for MnOx-(A)BC catalysts but no clear trend in structure-function relationship for their particular use in a given application could be established. The presence of biochar (as opposed to its absence) was noted to prevent aggregation of jacobsite nanoparticles in one publication [110]. More specifically, Hu et al. [84] mention the positive effect of N intrinsic to soybean dregs on photolytic degradation of synthetic dye Direct Green BE. Further than that, no comparison of different (A)BCs for any particular catalytic application was included in the dataset, therefore, no conclusions could be reached regarding activity and Mn oxidation state.

4.2.3. Catalysed oxidation/reduction of gas-phase pollutants

Key Insight 6: In the catalytic oxidation/reduction of gaseous pollutants, MnOx-(A)BCs often exhibit a dual catalyst/sorbent character. The preferred MnOx phase and synthesis depends on the desired catalysed reaction, but temperature resistance and resistance to poisoning are important factors for catalyst success, especially in flue gas settings and can be improved by the introduction of a second metal phase, such as iron or cerium.

MnOx-BCs are used to catalyse both reduction and oxidation reactions in the gas phase. **Selective catalytic reduction** is a standard mechanism to remove NO_x from car exhausts and stationary combustion plants such as thermal power stations and waste incinerators. While the most commonly used SCRs are vanadium or platinum based, inorganic MnOx are attractive low-temperature catalysts in SCRs as they have high activities at these temperatures, outperforming noble metal catalysts at a lower cost [41,116–118]. Rather than pH stability as in aquatic applications, temperature resistance plays an important role for this application. Degradation kinetics, degradation efficiency, performance in the presence of steam, SO_2 and others, as well as the possibility of catalyst regeneration are relevant parameters. MnOx have also been considered as alternatives to AC sorbents as they can form oxides with Hg species, such as Hg manganates. They are already employed to oxidise hydrocarbons, where the lattice oxygen serves as the oxidant via the Mars-Maessen mechanism [119], and researched for simultaneous SO_2 and Hg^0 oxidation [68]. Other possible applications include indoor **formaldehyde oxidation** at room temperature, which is a challenge for most transition metal catalysts which perform well above 80 °C [120]. It places importance on surface hydroxyl and chemisorbed oxygen groups of peracetic acid-activated carbon; in addition, the pore structure of BC precursor material (coconut fibre) and poorly crystalline δ-MnO_2 are specifically needed for sustained, successful HCHO removal. This provides a good illustration of an application optimising for both MnOx and (A)BC to achieve a successful product. Pierri et al. [45] conducted alkene epoxidation with different Mn^{2+}-biochars, finding that their biochar catalysts exhibited significantly faster reaction kinetics than SiO_2-based hybrid catalysts, showcasing that a cheap agro-waste feedstock may perform exceptionally well in this setting.

Although not always specified, manganese(IV) or mixed valences are often reported for deNOx applications. Yang et al.'s [39] mixed $Mn^{2+,3+,4+}$Ox-BC for flue gas desulfurisation indicated that the reaction was accompanied by a decrease in catalyst activity. They noted that the SO_2 oxidation may simultaneously oxidise the catalyst, as slightly higher MnO_2 XRD signatures were observed. This suggests that this reaction may, in fact, not be catalytic but a simple oxidation. Liu et al. [121] utilise a CoMn-BC composite for wet magnesia FGD. While the study focused on cobalt catalysts, it concluded that the addition of Mn lowers the price, as well as lowering cobalt leaching into the $MgSO_3$ solid product of the oxidation reaction. Other studies suggest that co-impregnation with cerium can greatly increase catalytic activity, as well as re-oxidising spent manganese(IV) on the MnOx-(A)BC surface (e.g. [116,117,122]). Many studies place an emphasis on the surface area of the MnOx-(A)BC, and chemical as well as physical activation is applied to optimise this parameter (e.g. Yang et al. [39]). Wet impregnation and deposition-precipitation are the dominant synthesis methods, and most samples are subjected to an anoxic heat treatment step, but no clear rationale for this could be found during data collection.

4.3. MnOx-ABC as sorbents

4.3.1. Material properties of MnOx-BC sorbents

Manganese oxide-modified biochars have shown great potential for sorption compared to other biochar modifications. For example, Lee and Shin [43] demonstrated the highest sorption capacities for Pb,

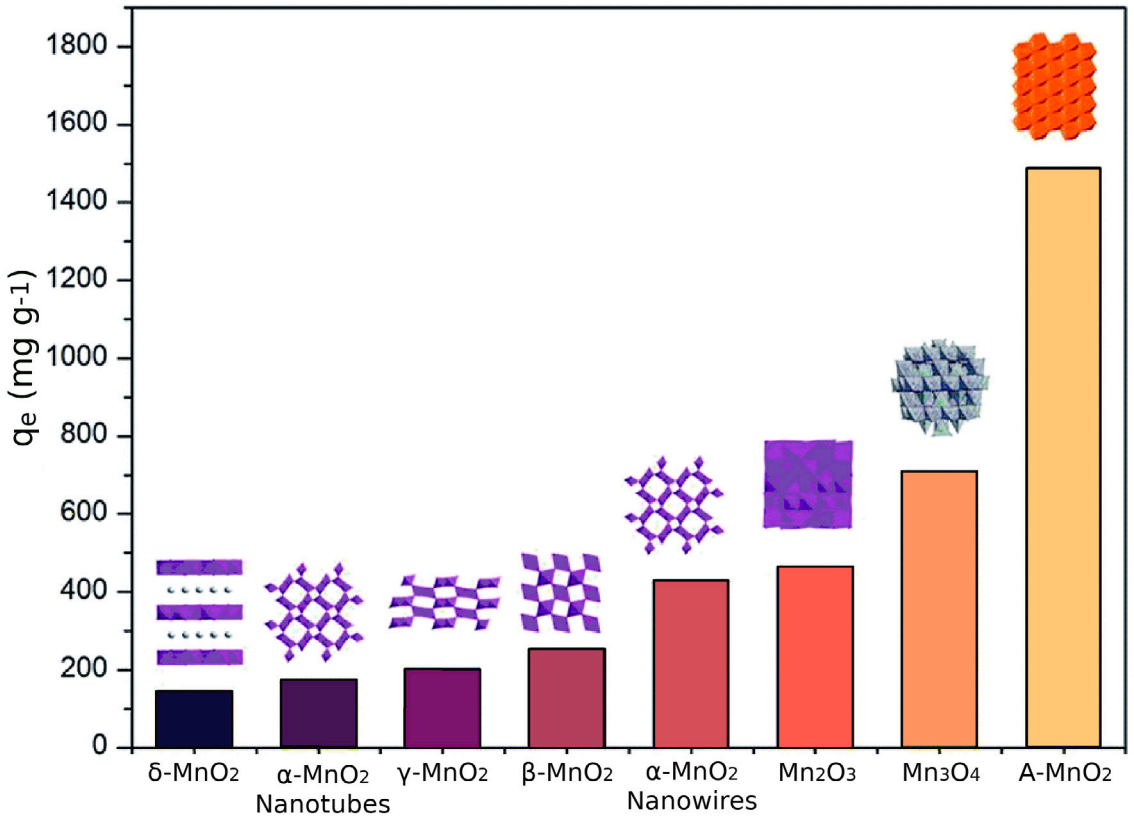

Fig. 2. Schematic illustration of sorption capacities of different pure MnOx for methyl orange. Modified from [115]. q_e : equilibrium sorption capacity, A-MnO_2 : amorphous MnO_2. Permission for reproduction still pending.

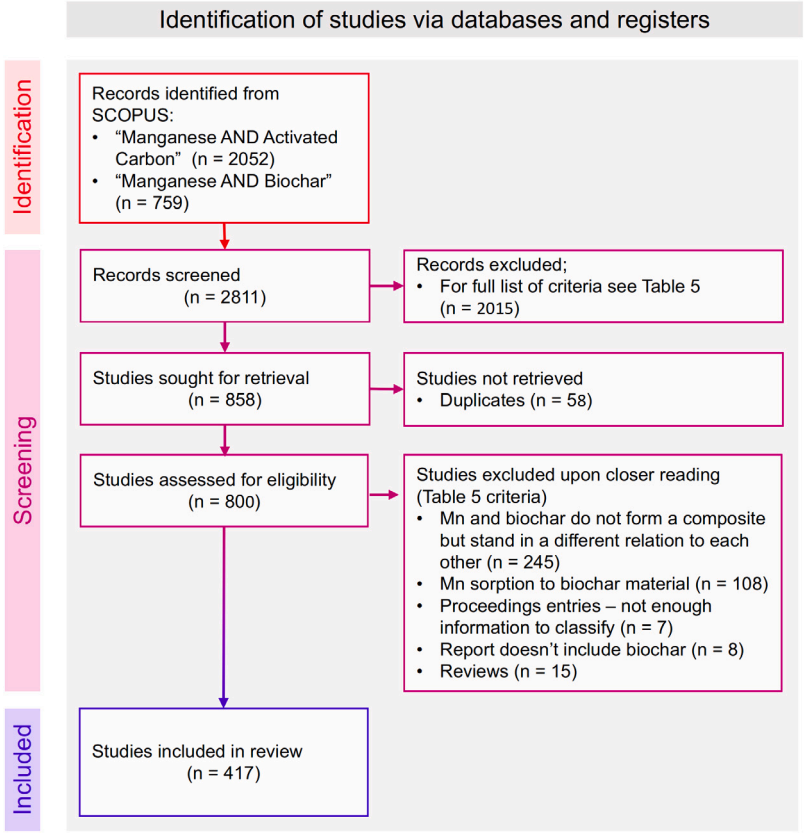

Fig. 3. Flow diagram of systematic review methodology, after [123].

Table 4
Use of different activation agents for biochars recorded in this literature review.

Activation agent	Frequency[a]
KOH	53
HCl	30
H_3PO_4	29
$KMnO_4$	26
HNO_3	17
$ZnCl_2$	12
steam	11
H_2SO_4	9
U|nknown	9
NaOH	7
CO_2	5
H_2O_2	5
K_2CO_3	5
NH_3	5
N_2	4
CH_3CO_3H	2
Others	9
Not specified	3

[a] Papers listed multiple times if several activation agents were applied.

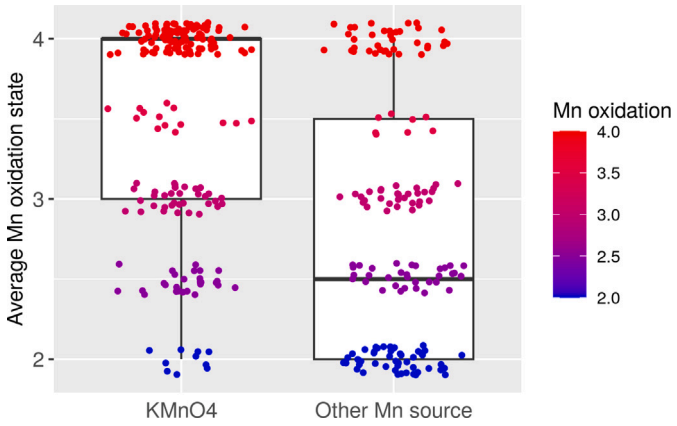

Fig. 4. Box plot of average Mn oxidation states in samples whose synthesis protocols included $KMnO_4$ (left, "$KMnO_4$") and samples where no $KMnO_4$ was applied (right, "Other Mn sources").

Cd and Zn on their $KMnO_4$-biochar composite compared to other biochar modifications. Sorption applications are extensively reviewed by [124]. They depend intricately on the interactions between sorbent and sorbate, which may be characterised as physisorption, ion-exchange, electrostatic interactions, complexation, redox interactions and others. These, in turn, are influenced by cation sizes, surface area and pore sizes, surface charge and cation exchange capacity. In addition, the environmental conditions surrounding the experiments, including pH conditions, temperature, and competing ions, have an effect (e.g. [125]), necessitating detailed characterisation of MnOx-BC sorbents. Maximum sorption capacity is commonly evaluated through batch sorption experiments resulting in sorption isotherms. Beyond that, the most frequently recorded material parameters are sorption kinetics, calculated thermodynamic parameters, pore volume, pore diameter and point of zero charge. Sorbents are exposed to a wide variety of potential environmental factors such as variations in pH, temperature, ionic strength of a solution, and competing pollutants to test the materials' selectivity for a certain substance. For some, especially organic, pollutants, there is significant overlap between the sorption and catalytic degradation of organic pollutants such as antibiotics and dyes. Plenty of reviews have been written on different MnOx and their applicability to sorption — for example on different manganese dioxides [126]. Fig. 2 demonstrates that the sorption capacities of different MnOx differ strongly — shown in this example for methyl orange dye [115].

4.3.2. *MnOx-(A)BC sorbents in the reviewed literature*

Key Insight 7: MnOx-(A)BCs are optimised for surface area, pore structure and often MnOx phase, in a composite where both MnOx and (A)BC display high sorption capacities in their own right. Still, there is much scope for fine-tuning the manganese valence, as well as biochar properties (more/less ordered, functional groups and bulk chemistry). Often, mixed Fe-Mn oxides are produced.

Sorption of environmental pollutants is the scientific field which has produced most MnOx-BC literature to date; With a majority of studies focusing on the sorption capacity of MnOx-BC on heavy metals from aqueous solution, a variety of pollutants including synthetic dyes, antibiotics other aqueous and gaseous pollutants are also addressed. MnOx-BC is also researched as a soil amendment where it is used to lower heavy metal and organic pollutant availability or toxicity to plants and its efficacy is evaluated in growth trials. Additionally, biochars may be the source of micronutrients and enhance productivity in growth trials [90]. Parameters for successful applications are surface area, porosity, surface functionality and charge of MnOx-(A)BCs, but practical aspects such as a low price, easy separation from the aqueous phase and regeneration of spent sorbent play in important role as well. While surface area and functionality are good predictors of a material's sorption capacity, the most successful manganese oxide phase cannot be generalised across applications and their performance is heavily dependent on the environmental conditions (pH, ionic strength, presence of competing ions, redox potential, temperature, etc.). Frequently, magnetic FeMn phases such as jacobsite are synthesised to aid the retrieval of the spent sorbent from a body of water. While in some cases, irreversible binding and inhibition of reduction/oxidation of toxic metals such as arsenic and chromium are desired, in other cases, the desorption of the pollutant and reusability of a sorbent are of primary concern and MnOx-(A)BC are tested for their stability in several weak acid washing cycles or, in the case of organic pollutants, heat treatment [37]. Further, there may be competition from non-target metals for sorption sites, which has to be taken into consideration. Sorption kinetics can also be a factor. Wan et al. [127] and [128] primarily studied the influence of pore size on sorption, determining that micropores were a *"key technical barrier limiting practical application of these hybrid adsorbents, particularly in high flow systems"*. Sorption applications have recently been reviewed by [124], where the performance of different MnOx-(A)BCs was evaluated and different synthesis procedures were described, for which there is no need for repetition, Instead, this section focuses on the diversity in manganese oxide phases and oxidation states applied in heavy metal sorption, focusing on chromium and arsenic as case studies.

Out of the three surveyed application areas, sorption literature is the only dataset where the majority of biochars did not undergo any physical or chemical activation procedure. Relationships between sorption behaviour of a particular aqueous substance and a biochar feedstock is very hard to draw, as evidenced by one study which showed no correlation between biochar feedstock and Cu(II) sorption capacity, suggesting that in this case, the manganese-containing oxide phase was the dominant factor in high sorption success [46].

The synthesised materials naturally depend on the target sorbent, but are not always characterised for Mn valence, and often mixed oxides, which is a common result of wet impregnation procedures (Fig. 7). Table 6 presents data on the MnOx-(A)BCs used in As, Pb, Cd, Cu, Cr sorption. Taking the example of **cadmium**, a large variation in sorption capacity by tested materials does not seem to correlate with manganese valence and BET surface area measurements — it appears necessary to take into account a larger set of factors to design an optimal sorbent, also taking into account experimental conditions.

Arsenic is the most comprehensively studied heavy metal in conjunction with MnOx-(A)BC sorbents. The toxicity of arsenite As^{3+} is

Table 5
Selected performance of MnOx-ABC based capacitors.

Composite	Biomass	Activation agent	Synthesis	Specific capacitance		Capacity retention		Energy density	Ref.
				at X [F g^{-1}]	X	over Y cycles [%]	Y	[Wh kg^{-1}]	
α-MnO_2-ABC	Wood	CO_2	ED	55.4–24.1	1–30 mA cm^{-1}	93	10000		[88]
MnO_2-ABC	Cotton stalk	H_3PO_4	PM	169	2A	99.2	500		[129]
MnO_2-ABC	Coconut shell	KOH, HCl	HT	522.7	5 mV				[98]
MnO_2-ABC	Bamboo	KOH, HCl	WI	158	10 mV s^{-1}				[97]
α-MnO_2-ABC	Coconut shell	KOH, HCl	WI	410.4	5 mV				[98]
α-MnO_2-ABC	Coconut shell	KOH, HCl	WI	479.2	5 mV				[98]
MnO_2-ABC	Citrus peel	KOH, HCl	HT	58	5 mV cm^{-2}	88	5000	20.37	[100]
α-MnO_2-ABC	Palm tree	KOH, HNO_3	HT	259	10 mV s^{-1}				[99]
MnO_2-ABC	T-shirt	NaF	ED	54.5	5 mV	97.5	1000	66.7	[33]
MnO_2-ABC	Wheat bran		HT	258	1 A	93.6	10000	32.6	[130]
MnO_2-ABC	Commercial AC and Lignin (separate)		HT			97.5	2000	14.11	[94]
MnO_2-ABC	Human hair		WI	291–410	5 mV s^{-1}				[32]

ED : electrochemical deposition, PM : physical dry mixing, HT : hydrothermal method, WI : wet impregnation, E. : energy, comm. : commercial.

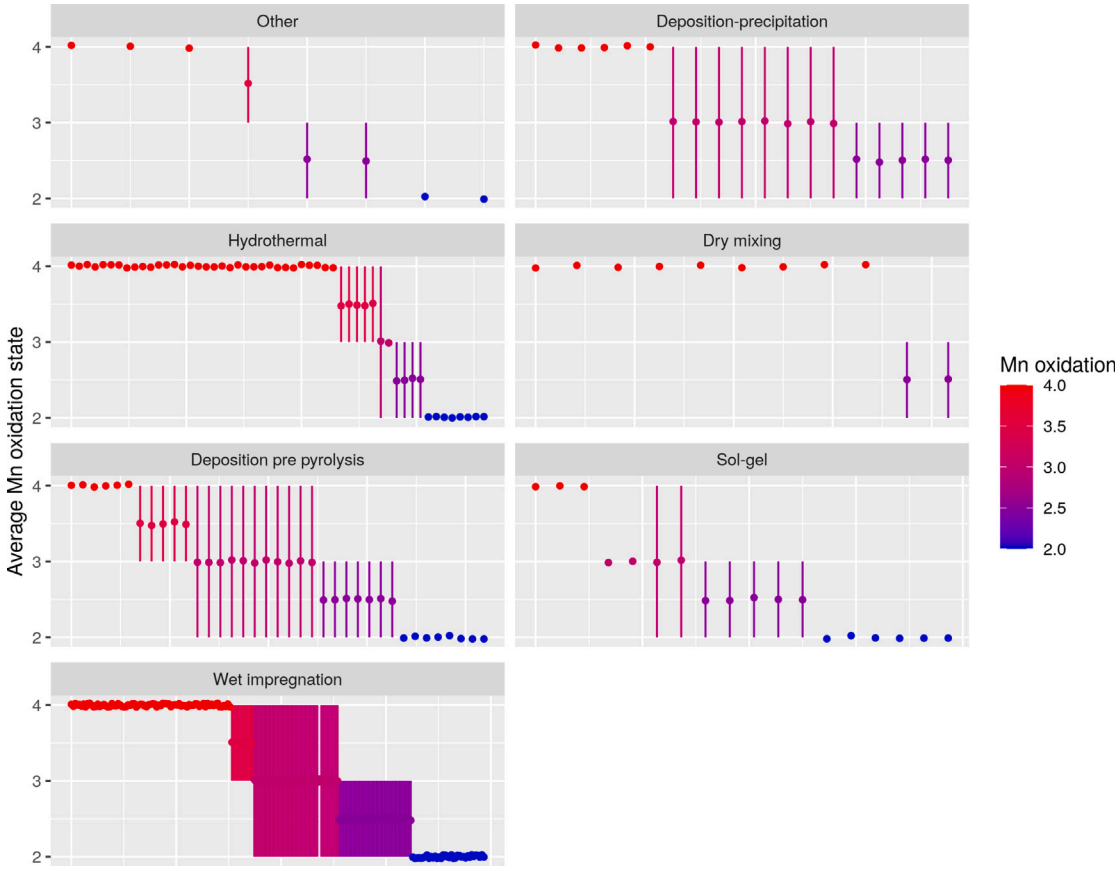

Fig. 5. Average oxidation states by synthesis method of the MnOx-BCs included in this study. "Other" category includes combustion synthesis, spray sorption, covalent grafting, pen lithography and studies where the synthesis method was not specified.

higher than that of arsenate As^{5+} and additionally, As^{5+} may be less mobile than As^{3+}, so the speciation of the element governs its environmental fate, toxicity and mobility [147]. Sorption of As cations in aqueous solutions depends on the solution pH, the involved MnOx, their mineral phase and Mn oxidation state. For example, it has been shown that As^{3+} oxidation by the $Mn^{3,4+}$ phyllomanganate birnessite occurs and Mn^{2+} is generated through the reaction, and that both Mn^{2+} and As^{5+} may subsequently be released into the aqueous phase or adsorbed to the mineral surface [148], causing passivation of the MnOx surface and slowing down oxidation. The formation of Mn^{2+}-As^{5+} precipitates has also been observed at higher pH values [149]. To summarise, the success of As^{3+} oxidation and subsequent sorption is highly dependent not only on the sorbent, but also on the pH conditions. Passivation of the sorbent might occur, so recycling studies on sorbents are imperative. Lin et al. not only looked at aqueous sorption of As^{3+} to FeMnOx-BC, but also at growth trials using paddy soil, where the growth in As-polluted soil, including criteria of plant healthy, enzymatic activity and As bioavailability [150], as well as As oxidation were studied. Despite expecting As^{3+} oxidation, Lin et al. only looked at produced and reported on reduced $Mn^{II,III}$ mixed oxides, citing Mn_3O_4 and Mn_2O_3 as likely Mn phases [133]. Other research groups [131,132] also studied Fe-$Mn^{II,III}$Ox-(A)BC and reported sorption of As^{5+}. As summarised in Table 6, the prepared sorbents vary widely in their maximum sorption capacity and surface area, but are fairly homogeneous in that they are $Mn^{II,II}$Ox, often mixed with Fe.

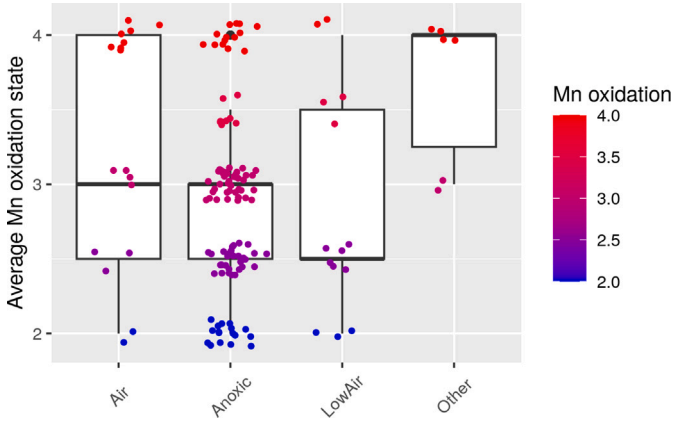

Fig. 6. Average manganese oxidation of reviewed papers after heat treatment with varying levels of oxygen content. Air : calcination in ventilated furnaces; Anoxic : calcinated in N_2, Ar, or other atmosphere specified as anoxic; LowAir : Calcination under O_2-limited conditions such as a muffle furnace or in a closed container; Other : unknown or other conditions (e.g. hydrothermal, but excluding hydrothermal synthesis, which is plotted in Fig. 5.).

Table 6
Selected sorption capacities of different MnOx-(A)BCs for the metal cations As^{3+}, As^{5+}, Pb^{2+}, Cd^{2+}, Cu^{2+}, Cr^{6+} and Cu^{2+}.

Composite type	Cation	Max. sorption capacity [mg g^{-1}]	S_{BET} [m^2 g^{-1}]	Ref
$FeMn^{II}$Ox-BC	As^{5+}	0.50	386.7	[131]
$Mn^{II}Fe_2O_4$-BC	As^{5+}	3.44	280.0	[131]
$FeMn^{II,III}$Ox-ABC	As^{5+}	16.84	741	[132]
$FeMn^{II,III}$Ox-BC	As^{3+}	8.25	208.6	[133]
$FeMn^{II,III}$Ox-BC	As	0.71	–	[134]
$LaFeMn^{II,III}$Ox-BC	As^{3+}	14.9	–	[134]
$LaFeMn^{II,III}$Ox-BC	As^{3+}	15.43	60.67	[135]
FeMnOx-BC	As	8.8	–	[136]
$Mn^{II,III}$Ox-BC	As	14.36	3.18	[137]
$Mn^{II,III}$Ox-BC	As^{5+}	0.59	–	[76]
Mn^{IV}Ox-BC	As^{5+}	0.91	–	[76]
$FeMn^{IV}$Ox-ABC	As^{5+}	1.11	124.4	[138]
MnOx-BC	Pb^{2+}	86.5	340	[49]
FeMnOx-HTC[a]	Pb^{2+}	99.5	138.5	[53]
$Mn^{II}Fe_2O_4$-BC	Pb^{2+}	39.61		[139]
$FeMn^{II,III}$Ox-BC	Pb^{2+}	154.9		[82]
$Mn^{II,III}$Ox-BC	Pb^{2+}	2.35	–	[76]
$Mn^{IV}O_2$-BC	Pb^{2+}	70.9	–	[140]
Mn^{IV}(?)Ox-BC	Pb^{2+}	66.14	364.7	[57]
Mn^{IV}Ox-BC	Pb^{2+}	47.05	–	[76]
$Mn^{II}Fe_2O_4$-BC	Cd^{2+}	23.32		[139]
MnOx-ABC	Cd^{2+}	12.21		[141]
$Mn^{II,III}$Ox-BC	Cd^{2+}	37.87	26.1	[142]
$Mn^{II,III}Fe_2O_4$Ox-BC	Cd^{2+}	127.8		[82]
$Mn^{II,III}Fe_2O_4$-BC	Cd^{2+}	181.5	30.4	[143]
$Mn^{IV}O_2$-BC	Cd^{2+}	84.76	–	[140]
Mn^{IV}Ox-BC	Cd^{2+}	> 112		[128]
$Mn^{II}Fe_2O_4$-BC	Cu^{2+}	29.08		[139]
MnOx-ABC	Cu^{2+}	39.48		[141]
δ-$Mn^{IV}O_2$-BC	Cu^{2+}	153.9		[144]
Mn^{IV}Ox-ABC	Cu^{2+}	> 248	513.4	[127]
Mn^{IV}(?)Ox-BC	Cu^{2+}	56.41	364.7	[57]
$FeMn^{II,III}$Ox-BC	Cr^{6+}	52.12	183.7	[145]
$FeMn^{4+}$Ox-BC	Cr^{6+}	31.02		[146]
$Mn^{II,III}Fe_2O_4$-BC	Sb^{3+}	237.5	30.4	[143]
Mn^{IV}Ox-ABC	Sb^{3+}	>126	513.4	[127]
Fe-2%Mn^{IV}Ox-BC	$Hg(0)_g$	0.004	288.8	[48]
Fe-2%Mn^{VII}Ox-BC	$Hg(0)_g$		158.5	[48]

[a] HTC : hydrothermal carbon.

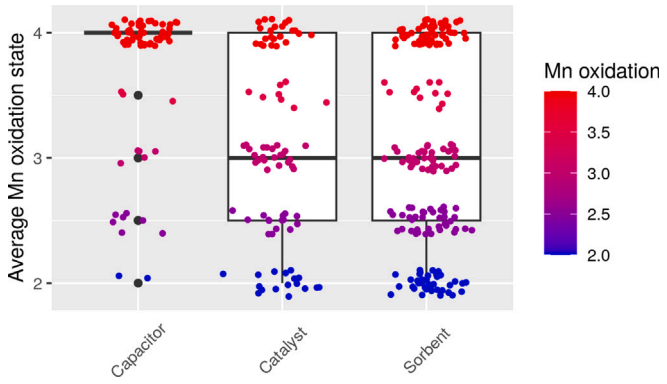

Fig. 7. Average manganese oxidation state of reviewed papers, according to application of the material as a capacitor, catalyst or sorbent.

5. Conclusions and future perspectives

This study reviews the manganese oxide - (activated) biochar composites (MnOx-(A)BC) across application areas. Both component phases – MnOx and (A)BC – are abundant and economic resources and their properties and performance vary across feedstocks and synthesis conditions, all of which can be strategically optimised. The means of biomass conversion into (A)BC exert significant influence on the porosity, polar functional groups, crystallinity of the carbon phase and (A)BC surface area. It has also been demonstrated that the morphological features of a feedstock can be retained to create advantageous pore structure under the right pyrolysis conditions. To truly optimise a MnOx-(A)BC sorbent/catalyst/capacitor, attention must also be paid to the manganese phase. Here, the choice of synthesis procedure is central, as the final porosity, surface area, crystallinity and nanomorphology of the MnOx phase depend it. Where facile and also cheap synthesis are prime objectives above process control, a variety of wet impregnation or simple physical mixing procedures are available. For greater control of the nanomorphology of the MnOx phase, hydrothermal protocols are favoured. The (A)BC phase can be expected to significantly influence the reaction parameters, so fine-tuning the manganese mineralogy is more complex than synthesising pure MnOx. Based on this review, the authors suggest that synthesis needs to be optimised on a case-by-case basis — either by comparing existing protocols across synthesis methods or desired material application. To facilitate this task, the supplement to this publication provides a database of all included publications and collected data on the biochar characteristics, MnOx characteristics, basic synthesis parameters and intended material applications.

5.1. Future perspectives

Before we can draw true synthesis-function relationships – either empirically or through a model – for the full spectrum of MnOx-(A)BC materials, across the full range of applications, there are still some major knowledge gaps and opportunities for further research:

Systematic comparisons. Screening studies for a particular application can help further the synthesis-function relationship only when a full rationalisation is given about the final material choice and synthesis parameters. Purely operational reasoning ('Material X had the highest sorption capacity for application A') does not suffice for this purpose. Systematic study of potential biochar feedstocks and their chemical and structural properties could lead to a synergy between traditional material sciences and biochar research communities. Some stand-out studies from this literature review were those which intentionally utilised the micro- and nanostructure of bio-based feestocks to the advantage of the final product.

Advanced analytical toolkits. In order to achieve a full understanding of synthesis-function relationships, it is necessary for future research to look beyond the standard analysis toolkit for inorganic materials such as MnOx. Firstly, the MnOx valence and crystal structure such as XRD do not always yield useful data, due to the interplay between the carbon phase and the MnOx phase reducing crystallinity and increasing dispersion on the (A)BC surface. Secondly, the nano- and micro-scale porous structure of biochar is varied dependent on feedstock and highly tunable with a diverse toolkit of activation protocols. Fully understanding the interplay between biochar, its activation and the performance of embedded MnOx will only be understood – and therefore optimised – with techniques such as X-ray tomography and X-ray Absorption Spectroscopy which capable of yielding detailed chemical, physical and structural information on materials without long-range order, such as MnOx-BC composites. Such in-depth studies would also be capable of progressing understanding of the impacts of minor mineral phases that are present in some biochar feedstocks, such as sewage sludge, which may for example alter pore morphology via pore narrowing or MnOx phase through catalytic transformations.

CRediT authorship contribution statement

Flora M. Brocza: Conceptualization, Data curation, Formal analysis, Investigation, Methodology, Validation, Visualization, Writing – original draft, Writing – review & editing. **Stella J. Foster:** Conceptualization, Data curation, Validation, Writing – original draft, Writing – review & editing. **Caroline L. Peacock:** Writing – review & editing, Supervision. **Jenny M. Jones:** Funding acquisition, Supervision, Writing – review & editing.

Acknowledgements

This work was supported by the RC-UK Centre for Doctoral Training in Bioenergy [Grant number EP/L014912/1]. The authors thank Bhoopesh Mishra for helpful early discussion.

Appendix A. Supplementary data

The data associated with this paper are openly available from the University of Leeds Data Repository: https://doi.org/10.5518/1307.

Supplementary material related to this article can be found online at https://doi.org/10.1016/j.biombioe.2024.107201.

References

[1] A. D'Harambue, IMnI Statistics 2019, International Manganese Institute, Paris, France, 2019, https://www.manganese.org/wp-content/uploads/2021/04/IMnI-2019-Annual-Review_ENG.pdf. Last accessed.

[2] Y. Tang, S. Zheng, Y. Xu, X. Xiao, H. Xue, H. Pang, Advanced batteries based on manganese dioxide and its composites, Energy Storage Mater. 12 (2018) 284–309, http://dx.doi.org/10.1016/j.ensm.2018.02.010.

[3] EBC, European Biochar Certificate - Guidelines for a Sustainable Production of Biochar 6.5E, European Biochar Foundation, 2018, http://dx.doi.org/10.13140/rg.2.1.4658.7043.

[4] N. Hagemann, K. Spokas, H.-P. Schmidt, R. Kägi, M. Böhler, T. Bucheli, Activated carbon, biochar and charcoal: Linkages and synergies across pyrogenic carbon's ABCs, Water 10 (2018) 182, http://dx.doi.org/10.3390/w10020182.

[5] D. Mohan, C.U. Pittman, P.H. Steele, Pyrolysis of wood/biomass for bio-oil: A critical review, Energy Fuels 20 (2006) 848–889, http://dx.doi.org/10.1021/ef0502397.

[6] O. Onay, O.M. Kockar, Slow fast and flash pyrolysis of rapeseed, Renew. Energy 28 (2003) 2417–2433, http://dx.doi.org/10.1016/s0960-1481(03)00137-x.

[7] H.S. Kambo, A. Dutta, A comparative review of biochar and hydrochar in terms of production, physico-chemical properties and applications, Renew. Sustain. Energy Rev. 45 (2015) 359–378, http://dx.doi.org/10.1016/j.rser.2015.01.050.

[8] S. Mandal, B. Sarkar, A.D. Igalavithana, Y.S. Ok, X. Yang, E. Lombi, N. Bolan, Mechanistic insights of 2,4-D sorption onto biochar: Influence of feedstock materials and biochar properties, Bioresour. Technol. 246 (2017) 160–167, http://dx.doi.org/10.1016/j.biortech.2017.07.073.

[9] O. Mašek, P. Brownsort, A. Cross, S. Sohi, Influence of production conditions on the yield and environmental stability of biochar, Fuel 103 (2013) 151–155, http://dx.doi.org/10.1016/j.fuel.2011.08.044.

[10] J.W. Gaskin, C. Steiner, K. Harris, K.C. Das, B. Bibens, Effect of low-temperature pyrolysis conditions on biochar for agricultural use, Trans. ASABE 51 (2008) 2061–2069, http://dx.doi.org/10.13031/2013.25409.

[11] Y. Chun, G. Sheng, C.T. Chiou, B. Xing, Compositions and sorptive properties of crop residue-derived chars, Environ. Sci. Technol. 38 (2004) 4649–4655, http://dx.doi.org/10.1021/es035034w.

[12] T. Iyobe, T. Asada, K. Kawata, K. Oikawa, Comparison of removal efficiencies for ammonia and amine gases between woody charcoal and activated carbon, J. Health Sci. 50 (2004) 148–153, http://dx.doi.org/10.1248/jhs.50.148.

[13] B. Singh, M. Camps-Arbestain, J. Lehmann (Eds.), Biochar: A Guide to Analytical Methods, Taylor and Francis Inc, 2017, https://www.ebook.de/de/product/28951494/biochar.html.

[14] T. Xie, K.R. Reddy, C. Wang, E. Yargicoglu, K. Spokas, Characteristics and applications of biochar for environmental remediation: A review, Crit. Rev. Environ. Sci. Technol. 45 (2015) 939–969, http://dx.doi.org/10.1080/10643389.2014.924180.

[15] C.T. Johnson, in: B. Singh, M. Camps-Arbestain, J. Lehmann (Eds.), Biochar: A Guide to Analytical Methods, Taylor and Francis Inc, 2017, pp. 199–212, https://www.ebook.de/de/product/28951494/biochar.html.

[16] G.C. Smith, in: B. Singh, M. Camps-Arbestain, J. Lehmann (Eds.), Biochar: A Guide to Analytical Methods, Taylor and Francis Inc, 2017, pp. 229–244, https://www.ebook.de/de/product/28951494/biochar.html.

[17] J. Kaal, R.C. Pereira, in: B. Singh, M. Camps-Arbestain, J. Lehmann (Eds.), Biochar: A Guide to Analytical Methods, Taylor and Francis Inc, 2017, pp. 170–186, https://www.ebook.de/de/product/28951494/biochar.html.

[18] R.J. Smernik, in: B. Singh, M. Camps-Arbestain, J. Lehmann (Eds.), Biochar: A Guide to Analytical Methods, Taylor and Francis Inc, 2017, pp. 151–161, https://www.ebook.de/de/product/28951494/biochar.html.

[19] P.S. Nico, T.Z. Regier, A.W. Gillespie, A.C. Cismasu, in: B. Singh, M. Camps-Arbestain, J. Lehmann (Eds.), Biochar: A Guide to Analytical Methods, Taylor and Francis Inc, 2017, pp. 23–38, https://www.ebook.de/de/product/28951494/biochar.html.

[20] L. Klüpfel, M. Keiluweit, M. Kleber, M. Sander, Redox properties of plant biomass-derived black carbon (biochar), Environ. Sci. Technol. 48 (2014) 5601–5611, http://dx.doi.org/10.1021/es500906d.

[21] F.G. Emmerich, C. Rettori, C.A. Luengo, ESR in heat treated carbons from the endocarp of babassu coconut, Carbon 29 (1991) 305–311, http://dx.doi.org/10.1016/0008-6223(91)90198-r.

[22] A. Prévoteau, F. Ronsse, I. Cid, P. Boeckx, K. Rabaey, The electron donating capacity of biochar is dramatically underestimated, Sci. Rep. 6 (2016) http://dx.doi.org/10.1038/srep32870.

[23] J.E. Post, Manganese oxide minerals: Crystal structures and economic and environmental significance, Proc. Natl. Acad. Sci. 96 (1999) 3447–3454, http://dx.doi.org/10.1073/pnas.96.7.3447.

[24] L. Qiao, M.T. Swihart, Solution-phase synthesis of transition metal oxide nanocrystals: Morphologies, formulae, and mechanisms, Adv. Colloid Interface Sci. 244 (2017) 199–266, http://dx.doi.org/10.1016/j.cis.2016.01.005.

[25] M. Villalobos, B. Toner, J. Bargar, G. Sposito, Characterization of the manganese oxide produced by pseudomonas putida strain MnB1, Geochim. Cosmochim. Acta 67 (2003) 2649–2662, http://dx.doi.org/10.1016/S0016-7037(03)00217-5.

[26] A. Biswal, B.C. Tripathy, K. Sanjay, T. Subbaiah, M. Minakshi, Electrolytic manganese dioxide (EMD): A perspective on worldwide production, reserves and its role in electrochemistry, RSC Adv. 5 (2015) 58255–58283, http://dx.doi.org/10.1039/c5ra05892.

[27] X. Wang, Y. Li, Synthesis and formation mechanism of manganese dioxide nanowires/nanorods., Chemistry 9 (2003) 300–306, http://dx.doi.org/10.1002/chem.200390024.

[28] S. Dharmarathna, S.L. Suib, Chapter 13. Porous cryptomelane-type manganese oxide octahedral molecular sieves (OMS-2)-synthesis, characterization and applications in catalysis, in: Catalysis Series, Royal Society of Chemistry, 2014, pp. 235–250, http://dx.doi.org/10.1039/9781782621034-00235.

[29] Z. Chen, Z. Jiao, D. Pan, Z. Li, M. Wu, C.-H. Shek, C.M.L. Wu, J.K.L. Lai, Recent advances in manganese oxide nanocrystals: Fabrication, characterization, and microstructure, Chem. Rev. 112 (2012) 3833–3855, http://dx.doi.org/10.1021/cr2004508.

[30] D. Moher, L. Shamseer, M. Clarke, D. Ghersi, A. Liberati, M. Petticrew, P. Shekelle, L.A. Stewart, Preferred reporting items for systematic review and meta-analysis protocols (PRISMA-P) 2015 statement, Syst. Rev. 4 (2015) http://dx.doi.org/10.1186/2046-4053-4-1.

[31] X. Shang, L. Yang, D. Ouyang, B. Zhang, W. Zhang, M. Gu, J. Li, M. Chen, L. Huang, L. Qian, Enhanced removal of 1 2 4-trichlorobenzene by modified biochar supported nanoscale zero-valent iron and palladium, Chemosphere 249 (2020) http://dx.doi.org/10.1016/j.chemosphere.2020.126518.

[32] D. Deng, B.-S. Kim, M. Gopiraman, I.S. Kim, Needle-like MnO_2/activated carbon nanocomposites derived from human hair as versatile electrode materials for supercapacitors, RSC Adv. 5 (2015) 81492–81498, http://dx.doi.org/10.1039/c5ra16624a.

[33] L. Bao, X. Li, Towards textile energy storage from cotton T-shirts, Adv. Mater. 24 (2012) 3246–3252, http://dx.doi.org/10.1002/adma.201200246.

[34] P. Ouředníček, B. Hudcová, L. Trakal, M. Pohořelý, M. Komárek, Synthesis of modified amorphous manganese oxide using low-cost sugars and biochars: Material characterization and metal(loid) sorption properties, Sci. Total Environ. 670 (2019) 1159–1169, http://dx.doi.org/10.1016/j.scitotenv.2019.03.300.

[35] F. Chacón, M. Cayuela, H. Cederlund, M. Sánchez-Monedero, Overcoming biochar limitations to remediate pentachlorophenol in soil by modifying its electrochemical properties, J. Hazard. Mater. 426 (2022) http://dx.doi.org/10.1016/j.jhazmat.2021.127805.

[36] Y. Qiu, Q. Zhang, Z. Wang, B. Gao, Z. Fan, M. Li, H. Hao, X. Wei, M. Zhong, Degradation of anthraquinone dye reactive blue 19 using persulfate activated with Fe/Mn modified biochar: Radical/non-radical mechanisms and fixed-bed reactor study, Sci. Total Environ. 758 (2021) http://dx.doi.org/10.1016/j.scitotenv.2020.143584.

[37] J. Li, L. Pan, G. Yu, C. Li, S. Xie, Y. Wang, Synthesis of an easily recyclable and safe adsorbent from sludge pyrochar for ciprofloxacin adsorption, Environ. Res. 192 (2021) http://dx.doi.org/10.1016/j.envres.2020.110258.

[38] P. Maneechakr, S. Karnjanakom, Environmental surface chemistries and adsorption behaviors of metal cations (Fe3+, Fe2+, Ca2+ and Zn2+) on manganese dioxide-modified green biochar, RSC Adv. 9 (2019) 24074–24086, http://dx.doi.org/10.1039/c9ra03112j.

[39] L. Yang, T. Huang, X. Jiang, W. Jiang, Effect of steam and CO_2 activation on characteristics and desulfurization performance of pyrolusite modified activated carbon, Adsorption 22 (2016) 1099–1107, http://dx.doi.org/10.1007/s10450-016-9832-7.

[40] J. Liao, L. Ding, Y. Zhang, W. Zhu, Efficient removal of uranium from wastewater using pig manure biochar: Understanding adsorption and binding mechanisms, J. Hazard. Mater. 423 (2022) http://dx.doi.org/10.1016/j.jhazmat.2021.127190.

[41] C. Yu, H. Wang, M. Lu, F. Zhu, Y. Yang, H. Huang, C. Zou, J. Xiong, Z. Zhong, Application of rice straw, corn cob, and lotus leaf as agricultural waste derived catalysts for low temperature SCR process: Optimization of preparation process, catalytic activity and characterization, Aerosol Air Qual. Res. 20 (2020) 862–876, http://dx.doi.org/10.4209/aaqr.2019.11.0596.

[42] Y. Liu, X. Zheng, S. Zhang, S. Sun, Enhanced removal of ibuprofen by heterogeneous photo-fenton-like process over sludge-based Fe_3O_4-MnO_2 catalysts, Water Sci. Technol. 85 (2022) 291–304, http://dx.doi.org/10.2166/wst.2021.612.

[43] H.-S. Lee, H.-S. Shin, Competitive adsorption of heavy metals onto modified biochars: Comparison of biochar properties and modification methods, J. Environ. Manag. 299 (2021) http://dx.doi.org/10.1016/j.jenvman.2021.113651.

[44] Lalhmunsiama, S.M. Lee, D. Tiwari, Manganese oxide immobilized activated carbons in the remediation of aqueous wastes contaminated with copper(II) and lead(II), Chem. Eng. J. 225 (2013) 128–137, http://dx.doi.org/10.1016/j.cej.2013.03.083.

[45] L. Pierri, A. Gemenetzi, A. Mavrogiorgou, J. Borges Regitano, Y. Deligiannakis, M. Louloudi, Biochar as supporting material for heterogeneous Mn(II) catalysts: Efficient olefins epoxidation with H2O2, Mol. Catal. 489 (2020) http://dx.doi.org/10.1016/j.mcat.2020.110946.

[46] W.-H. Huang, R.-M. Wu, J.-S. Chang, S.-Y. Juang, D.-J. Lee, Pristine and manganese ferrite modified biochars for copper ion adsorption: Type-wide comparison, Bioresour. Technol. 360 (2022) http://dx.doi.org/10.1016/j.biortech.2022.127529.

[47] G. Wu, T.-S. Jeong, C.-H. Won, L. Cui, Comparison of catalytic ozonation of phenol by activated carbon and manganese-supported activated carbon prepared from brewing yeast, Korean J. Chem. Eng. 27 (2010) 168–173, http://dx.doi.org/10.1007/s11814-009-0337-x.

[48] L. Jia, B.-G. Fan, Y.-X. Yao, F. Han, R.-P. Huo, C.-W. Zhao, Y. Jin, Study on the elemental mercury adsorption characteristics and mechanism of iron-based modified biochar materials, Energy Fuels 32 (2018) 12554–12566, http://dx.doi.org/10.1021/acs.energyfuels.8b02890.

[49] Faheem, H. Yu, J. Liu, J. Shen, X. Sun, J. Li, L. Wang, Preparation of MnOx -loaded biochar for Pb 2+ removal: Adsorption performance and possible mechanism, J. Taiwan Inst. Chem. Eng. 66 (2016) 313–320, http://dx.doi.org/10.1016/j.jtice.2016.07.010.

[50] M.C. Wang, G.D. Sheng, Y.P. Qiu, A novel manganese-oxide/biochar composite for efficient removal of lead(II) from aqueous solutions, Int. J. Environ. Sci. Technol. 12 (2015) 1719–1726, http://dx.doi.org/10.1007/s13762-014-0538-7.

[51] U. Kamran, S.-J. Park, MnO_2-decorated biochar composites of coconut shell and rice husk: An efficient lithium ions adsorption–desorption performance in aqueous media, Chemosphere 260 (2020) http://dx.doi.org/10.1016/j.chemosphere.2020.127500.

[52] J. Shim, M. Kumar, R. Goswami, P. Mazumder, B.-T. Oh, P.J. Shea, Removal of p-cresol and tylosin from water using a novel composite of alginate recycled, MnO_2 and activated carbon, J. Hazard. Mater. 364 (2019) 419–428, http://dx.doi.org/10.1016/j.jhazmat.2018.09.065.

[53] Z. Niu, W. Feng, H. Huang, B. Wang, L. Chen, Y. Miao, S. Su, Green synthesis of a novel Mn–Zn ferrite/biochar composite from waste batteries and pine sawdust for Pb2+ removal, Chemosphere 252 (2020) http://dx.doi.org/10.1016/j.chemosphere.2020.126529.

[54] S. Pradhan, V. Somkuwar, N. Jha, Waste to energy application of sweet lime derived carbon with δ-MnO_2 for zinc ion battery, Mater. Today: Proc. 66 (2022) 2513–2520.

[55] C. Liu, Z. Tang, Y. Chen, S. Su, W. Jiang, Characterization of mesoporous activated carbons prepared by pyrolysis of sewage sludge with pyrolusite, Bioresour. Technol. 101 (2010) 1097–1101, http://dx.doi.org/10.1016/j.biortech.2009.09.012.

[56] L. Fan, J. Chen, J. Guo, X. Jiang, W. Jiang, Influence of manganese, iron and pyrolusite blending on the physiochemical properties and desulfurization activities of activated carbons from walnut shell, J. Anal. Appl. Pyrolysis 104 (2013) 353–360, http://dx.doi.org/10.1016/j.jaap.2013.06.014.

[57] R. Xie, W. Jiang, L. Wang, J. Peng, Y. Chen, Effect of pyrolusite loading on sewage sludge-based activated carbon in Cu(II), Pb(II), and Cd(II) adsorption, Environ. Prog. Sustain. Energy 32 (2013) 1066–1073, http://dx.doi.org/10.1002/ep.11710.

[58] Y. Chen, W. Jiang, L. Jiang, X. Ji, Adsorption behavior of activated carbon derived from pyrolusite-modified sewage sludge: Equilibrium modeling, kinetic and thermodynamic studies, Water Sci. Technol. 64 (2011) 661–669, http://dx.doi.org/10.2166/wst.2011.670.

[59] C.-M. Hung, C.-P. Huang, C.-W. Chen, C.-H. Wu, Y.-L. Lin, C.-D. Dong, Activation of percarbonate by water treatment sludge–derived biochar for the remediation of PAH-contaminated sediments, Environ. Pollut. 265 (2020) http://dx.doi.org/10.1016/j.envpol.2020.114914.

[60] M. Li, Z. He, H. Zhong, W. Sun, M. Ye, Y. Zhou, A novel multi-components hierarchical porous composite prepared from solid wastes for benzohydroxamic acid degradation, J. Colloid Interface Sci. 630 (2023) 714–726, http://dx.doi.org/10.1016/j.jcis.2022.10.124.

[61] P. Cui, C. Liu, X. Su, Q. Yang, L. Ge, M. Huang, F. Dang, T. Wu, Y. Wang, Atomically dispersed manganese on biochar derived from a hyperaccumulator for photocatalysis in organic pollution remediation, Environ. Sci. Technol. 56 (2022) 8034–8042, http://dx.doi.org/10.1021/acs.est.2c00992.

[62] P. Wu, P. Cui, Y. Zhang, M.E. Alves, C. Liu, D. Zhou, Y. Wang, Unraveling the molecular mechanisms of Cd sorption onto MnOx-loaded biochar produced from the Mn-hyperaccumulator phytolacca americana, J. Hazard. Mater. 423 (2022) http://dx.doi.org/10.1016/j.jhazmat.2021.127157.

[63] X. Wang, P. Zhang, C. Wang, H. Jia, X. Shang, J. Tang, H. Sun, Metal-rich hyperaccumulator-derived biochar as an efficient persulfate activator: Role of intrinsic metals (Fe, Mn and Zn) in regulating characteristics, performance and reaction mechanisms, J. Hazard. Mater. 424 (2022) http://dx.doi.org/10.1016/j.jhazmat.2021.127225.

[64] H. Fu, S. Ma, P. Zhao, S. Xu, S. Zhan, Activation of peroxymonosulfate by graphitized hierarchical porous biochar and $MnFe_2o_4$ magnetic nanoarchitecture for organic pollutants degradation: Structure dependence and mechanism, Chem. Eng. J. 360 (2019) 157–170, http://dx.doi.org/10.1016/j.cej.2018.11.207.

[65] X. Liu, G. Zhang, L. Lin, Z.H. Khan, W. Qiu, Z. Song, Synthesis and characterization of novel Fe-Mn-Ce ternary oxide-biochar composites as highly efficient adsorbents for as(III) removal from aqueous solutions, Materials 11 (2018) http://dx.doi.org/10.3390/ma11122445.

[66] H. Li, C.-Y. Wu, Y. Li, L. Li, Y. Zhao, J. Zhang, Role of flue gas components in mercury oxidation over TiO_2 supported MnOx-CeO_2 mixed-oxide at low temperature, J. Hazard. Mater. 243 (2012) 117–123.

[67] G. Qi, R.T. Yang, R. Chang, MnOx-CeO_2 mixed oxides prepared by co-precipitation for selective catalytic reduction of NO with NH3 at low temperatures, Appl. Catal. B 51 (2004) 93–106, http://dx.doi.org/10.1016/j.apcatb.2004.01.023.

[68] W. Yang, Y. Liu, Q. Wang, J. Pan, Removal of elemental mercury from flue gas using wheat straw chars modified by Mn-Ce mixed oxides with ultrasonic-assisted impregnation, Chem. Eng. J. 326 (2017) 169–181, http://dx.doi.org/10.1016/j.cej.2017.05.106.

[69] S. Shu, J.-X. Guo, X.-L. Liu, X.-J. Wang, H.-Q. Yin, D.-M. Luo, Effects of pore sizes and oxygen-containing functional groups on desulfurization activity of Fe/NAC prepared by ultrasonic-assisted impregnation, Appl. Surf. Sci. 360 (2016) 684–692, http://dx.doi.org/10.1016/j.apsusc.2015.11.046.

[70] Q. Feng, L. Liu, K. Yanagisawa, Effects of synthesis parameters on the formation of birnessite-type manganese oxides, J. Mater. Sci. Lett. 19 (2000) 1567–1570, http://dx.doi.org/10.1023/A:1006733308073.

[71] Y.-J. Shih, Y.-R. Chen, C.-L. Chen, J.-Y. Lin, C.-P. Huang, The electrosorption characteristics of simple aqueous ions on loofah-derived activated carbon decorated with manganese dioxide polymorphs: The effect of pseudocapacitance and beyond, Chem. Eng. J. 425 (2021) http://dx.doi.org/10.1016/j.cej.2021.130606.

[72] X. Xiao, Y. Wang, G. Chen, L. Wang, Y. Wang, Mn_3O_4/activated carbon composites with enhanced electrochemical performances for electrochemical capacitors, J. Alloys Compd. 703 (2017) 163–173, http://dx.doi.org/10.1016/j.jallcom.2017.01.272.

[73] F. Cheng, J. Zhao, W. Song, C. Li, H. Ma, J. Chen, P. Shen, Facile controlled synthesis of MnO_2 nanostructures of novel shapes and their application in batteries, Inorg. Chem. 45 (2006) 2038–2044, http://dx.doi.org/10.1021/ic051715b.

[74] W. Tian, H. Yang, X. Fan, X. Zhang, Catalytic reduction of NOx with NH_3 over different-shaped MnO2 at low temperature, J. Hazard. Mater. 188 (2011) 105–109, http://dx.doi.org/10.1016/j.jhazmat.2011.01.078.

[75] L. Zhang, X. Liu, X. Huang, W. Wang, P. Sun, Y. Li, Adsorption of Pb^{2+} from aqueous solutions using Fe–Mn binary oxides-loaded biochar: Kinetics, isotherm and thermodynamic studies, Environ. Technol. 40 (2019) 1853–1861, http://dx.doi.org/10.1080/09593330.2018.1432693.

[76] S. Wang, B. Gao, Y. Li, A. Mosa, A.R. Zimmerman, L.Q. Ma, W.G. Harris, K.W. Migliaccio, Manganese oxide-modified biochars: Preparation, characterization, and sorption of arsenate and lead, Bioresour. Technol. 181 (2015) 13–17, http://dx.doi.org/10.1016/j.biortech.2015.01.044.

[77] R.M. McKenzie, The adsorption of lead and other heavy metals on oxides of manganese and iron, Aust. J. Soil Res. 18 (1980) 61–73.

[78] X. Ma, W. Zhou, Y. Chen, Structure and photocatalytic properties of Mn-doped TiO_2 loaded on wood-based activated carbon fiber composites, Materials 10 (2017) 65–69, http://dx.doi.org/10.3390/ma10060631.

[79] D. Li, Y. Chen, F. Yin, L. Zhu, J. Li, X. Ma, Facile synthesis of Mn/N-doped TiO_2 on wood-based activated carbon fiber as an efficient visible-light-driven photocatalyst, J. Mater. Sci. 53 (2018) 11671–11683, http://dx.doi.org/10.1007/s10853-018-2429-7.

[80] X. Ma, Y. Chen, Preparation and characterization of Mn/N Co-doped TiO2 loaded on wood-based activated carbon fiber and its visible light photodegradation, Polymers 7 (2015) 1660–1673, http://dx.doi.org/10.3390/polym7091476.

[81] L. Trakal, Z. Michálková, L. Beesley, M. Vítková, P. Ouředníček, A. Barceló, V. Ettler, S. Číhalová, M. Komárek, AMOchar: Amorphous manganese oxide coating of biochar improves its efficiency at removing metal(loid)s from aqueous solutions, Sci. Total Environ. 625 (2018) 71–78, http://dx.doi.org/10.1016/j.scitotenv.2017.12.267.

[82] L. Zhang, J. Guo, X. Huang, W. Wang, P. Sun, Y. Li, J. Han, Functionalized biochar-supported magnetic $MnFe_2O_4$ nanocomposite for the removal of Pb(II) and Cd(II), RSC Adv. 9 (2019) 365–376, http://dx.doi.org/10.1039/c8ra09061k.

[83] Z. Xiao, L. Zhang, L. Wu, D. Chen, Adsorptive removal of Cu(II) from aqueous solutions using a novel macroporous bead adsorbent based on poly(vinyl alcohol)/sodium alginate/$KMnO_4$ modified biochar, J. Taiwan Inst. Chem. Eng. 102 (2019) 110–117, http://dx.doi.org/10.1016/j.jtice.2019.05.010.

[84] J. Hu, L. Zhang, B. Lu, X. Wang, H. Huang, $LaMnO_3$ nanoparticles supported on N doped porous carbon as efficient photocatalyst, Vacuum 159 (2019) 59–68, http://dx.doi.org/10.1016/j.vacuum.2018.10.021.

[85] M. Si, Z.F. Wang, W. Ji, G. Yang, L.S. Liu, J.X. Wu, E. Wang, X. Gou, Comparison of De-NOX performance of Mn/AC and Mn/Bio-char on low-temperature SCR, Appl. Mech. Mater. 694 (2014) 484–488, http://dx.doi.org/10.4028/www.scientific.net/AMM.694.484.

[86] A. Bello, D.M. Sanni, S.A. Adeniji, V. Anye, K. Orisekeh, M. Kigozi, R. Koech, Combustion synthesis of battery-type positive electrodes for robust aqueous hybrid supercapacitor, J. Energy Storage 27 (2020) http://dx.doi.org/10.1016/j.est.2019.101160.

[87] H. Huang, W. Liang, R. Li, A. Ali, X. Zhang, R. Xiao, Z. Zhang, M.K. Awasthi, D. Du, P. Dang, D. Huang, Converting spent battery anode waste into a porous biocomposite with high Pb(II) ion capture capacity from solution, J. Clean. Prod. 184 (2018) 622–631, http://dx.doi.org/10.1016/j.jclepro.2018.03.017.

[88] C. Chen, Y. Zhang, Y. Li, J. Dai, J. Song, Y. Yao, Y. Gong, I. Kierzewski, J. Xie, L. Hu, All-wood, low tortuosity, aqueous, biodegradable supercapacitors with ultra-high capacitance, Energy Environ. Sci. 10 (2017) 538–545, http://dx.doi.org/10.1039/c6ee03716.

[89] H.R. Kim, J.H. Lee, S.K. Lee, Y. Chun, C. Park, J.-H. Jin, H.U. Lee, S.W. Kim, Fabricating a modified biochar-based all-solid-state flexible microsupercapacitor using pen lithography, J. Clean. Prod. 284 (2021) http://dx.doi.org/10.1016/j.jclepro.2020.125449.

[90] D. Skrzypczak, D. Szopa, K. Mikula, G. Izydorczyk, S. Baśladyńska, V. Hoppe, K. Pstrowska, Z. Wzorek, H. Kominko, M. Kulazyński, K. Moustakas, K. Chojnacka, A. Witek-Krowiak, Tannery waste-derived biochar as a carrier of micronutrients essential to plants, Chemosphere 294 (2022) http://dx.doi.org/10.1016/j.chemosphere.2022.133720.

[91] B. Deljoo, H. Tan, S.L. Suib, M. Aindow, Thermally activated structural transformations in manganese oxide nanoparticles under air and argon atmospheres, J. Mater. Sci. 55 (2020) 7247–7258, http://dx.doi.org/10.1007/s10853-020-04525-6.

[92] B.E. Conway, Electrochemical Supercapacitors, Springer US, Boston, MA, 1999.

[93] S.W. Zhang, G.Z. Chen, Manganese oxide based materials for supercapacitors, Energy Mater. 3 (2008) 186–200, http://dx.doi.org/10.1179/174892409x427940.

[94] S. Jha, S. Mehta, Y. Chen, L. Ma, P. Renner, D.Y. Parkinson, H. Liang, Design and synthesis of lignin-based flexible supercapacitors, ACS Sustain. Chem. Eng. 8 (2020) 498–511, http://dx.doi.org/10.1021/acssuschemeng.9b05880.

[95] W. Wei, X. Cui, W. Chen, D.G. Ivey, Manganese oxide-based materials as electrochemical supercapacitor electrodes, Chem. Soc. Rev. 40 (2011) 1697–1721, http://dx.doi.org/10.1039/c0cs00127a.

[96] D. Wu, X. Xie, Y. Zhang, D. Zhang, W. Du, X. Zhang, B. Wang, MnO2/carbon composites for supercapacitor: Synthesis and electrochemical performance, Front. Mater. 7 (2020) http://dx.doi.org/10.3389/fmats.2020.00002.

[97] R. Zhuang, L. Xu, D. Li, N. Muhammad, J. Chen, Y. Yu, H. Song, J. Ma, X. Liu, X. Chen, Acidified bamboo-derived activated carbon/manganese dioxide composite as a high-performance electrode material for capacitive deionization, Int. J. Electrochem. Sci. 15 (2020) 3104–3118, http://dx.doi.org/10.20964/2020.04.23.

[98] J. Adorna, M.G. Borines, R.-A. Doong, Capacitive deionization utilizing activated biochar - manganese dioxide (AB - MD) nanocomposites for desalination applications, in: IOP Conference Series: Materials Science and Engineering, 2020, http://dx.doi.org/10.1088/1757-899X/778/1/012161.

[99] B. Govindan, E. Alhseinat, I.F.F. Darawsheh, I. Ismail, K. Polychronopoulou, M.A. Jaoude, A.F. Arangadi, F. Banat, Activated carbon derived from Phoenix dactylifera (palm tree) and decorated with MnO 2 nanoparticles for enhanced hybrid capacitive deionization electrodes, ChemistrySelect 5 (2020) 3248–3256, http://dx.doi.org/10.1002/slct.201901358.

[100] M. Fan, X. Zeng, X. Yang, X. Zhang, B. Ren, Rational design of asymmetric supercapacitors via a hierarchical core–shell nanocomposite cathode and biochar anode, RSC Adv. 9 (2019) 42543–42553, http://dx.doi.org/10.1039/c9ra09142d.

[101] H. Wei, X. Wang, D. Zhang, W. Du, X. Sun, F. Jiang, T. Shi, Facile synthesis of lotus seedpod-based 3D hollow porous activated carbon/manganese dioxide composite for supercapacitor electrode, J. Electroanal. Soc. 853 (2019) 618–627, http://dx.doi.org/10.1016/j.jelechem.2019.113561.

[102] P.H. Wadekar, R.V. Khose, D.A. Pethsangave, S. Some, Waste-derived heteroatom-doped activated carbon/manganese dioxide trio-composite for supercapacitor applications, Energy Technol. 8 (2020) http://dx.doi.org/10.1002/ente.201901402.

[103] S. Ristig, N. Cibura, J. Strunk, Manganese oxides in heterogeneous (photo)catalysis: Possibilities and challenges, Green 5 (2015) http://dx.doi.org/10.1515/green-2015-0010.

[104] D. Murzin, Engineering Catalysis, De Gruyter, 2013, http://dx.doi.org/10.1515/9783110283372.

[105] J.R. Carney, B.R. Dillon, S.P. Thomas, Recent advances of manganese catalysis for organic synthesis, Eur. J. Org. Chem. 2016 (2016) 3912–3929, http://dx.doi.org/10.1002/ejoc.201600018.

[106] D. Jia, K. Hanna, G. Mailhot, M. Brigante, A review of manganese(III) (oxyhydr)oxides use in advanced oxidation processes, Molecules 26 (2021) 5748, http://dx.doi.org/10.3390/molecules26195748.

[107] S. Zhang, B. Zhang, B. Liu, S. Sun, A review of Mn-containing oxide catalysts for low temperature selective catalytic reduction of NOx with NH3: Reaction mechanism and catalyst deactivation, RSC Adv. 7 (2017) 26226–26242, http://dx.doi.org/10.1039/c7ra03387g.

[108] J. Nawrocki, B. Kasprzyk-Hordern, The efficiency and mechanisms of catalytic ozonation, Appl. Catal. B 99 (2010) 27–42, http://dx.doi.org/10.1016/j.apcatb.2010.06.033.

[109] F. Mao, in: S.K. Ong, R.Y. Surampalli, A. Bhandari, P. Champagne, R.D. Tyagi, I. Lo (Eds.), Natural Processes and Systems for Hazardous Waste Treatment, American Society of Civil Engineers, 2008, pp. 120–161.

[110] C. Lai, F. Huang, G. Zeng, D. Huang, L. Qin, M. Cheng, C. Zhang, B. Li, H. Yi, S. Liu, L. Li, L. Chen, Fabrication of novel magnetic $MnFe_2O_4$/bio-char composite and heterogeneous photo-Fenton degradation of tetracycline in near neutral pH, Chemosphere 224 (2019) 910–921, http://dx.doi.org/10.1016/j.chemosphere.2019.02.193.

[111] L. Li, C. Lai, F. Huang, M. Cheng, G. Zeng, D. Huang, B. Li, S. Liu, M. Zhang, L. Qin, M. Li, J. He, Y. Zhang, L. Chen, Degradation of naphthalene with magnetic bio-char activate hydrogen peroxide: Synergism of bio-char and Fe–Mn binary oxides, Water Res. 160 (2019) 238–248, http://dx.doi.org/10.1016/j.watres.2019.05.081.

[112] Y. Huang, Y. Sun, Z. Xu, M. Luo, C. Zhu, L. Li, Removal of aqueous oxalic acid by heterogeneous catalytic ozonation with MnOx/sewage sludge-derived activated carbon as catalysts, Sci. Total Environ. 575 (2017) 50–57, http://dx.doi.org/10.1016/j.scitotenv.2016.10.026.

[113] H. Zhou, X. Zhu, B. Chen, Magnetic biochar supported α-MnO_2 nanorod for adsorption enhanced degradation of 4-chlorophenol via activation of peroxydisulfate, Sci. Total Environ. 724 (2020) http://dx.doi.org/10.1016/j.scitotenv.2020.138278.

[114] H. Hao, Q. Zhang, Y. Qiu, L. Meng, X. Wei, W. Sang, J. Tao, Insight into the degradation of orange g by persulfate activated with biochar modified by iron and manganese oxides: Synergism between Fe and Mn, J. Water Process Eng. 37 (2020) http://dx.doi.org/10.1016/j.jwpe.2020.101470.

[115] Y. Liu, J. Wei, Y. Tian, S. Yan, The structure–property relationship of manganese oxides: Highly efficient removal of methyl orange from aqueous solution, J. Mater. Chem. A 3 (2015) 19000–19010, http://dx.doi.org/10.1039/c5ta05507e.

[116] Y. Shu, F. Zhang, H. Wang, Manganese-cerium mixed oxides supported on rice husk based activated carbon with high sulfur tolerance for low temperature selective catalytic reduction of nitrogen oxides with ammonia, RSC Adv. 9 (2019) 23964–23972, http://dx.doi.org/10.1039/c9ra03937f.

[117] B. Shen, J. Chen, S. Yue, G. Li, A comparative study of modified cotton biochar and activated carbon based catalysts in low temperature SCR, Fuel 156 (2015) 47–53, http://dx.doi.org/10.1016/j.fuel.2015.04.027.

[118] L. Gao, C. Li, S. Li, W. Zhang, X. Du, L. Huang, Y. Zhu, Y. Zhai, G. Zeng, Superior performance and resistance to SO_2 and H_2O over CoOx-modified MnOx/biomass activated carbons for simultaneous Hg0 and NO removal, Chem. Eng. J. 371 (2019) 781–795, http://dx.doi.org/10.1016/j.cej.2019.04.104.

[119] E.J. Granite, H.W. Pennline, R.A. Hargis, Novel sorbents for mercury removal from flue gas, Ind. Eng. Chem. Res. 39 (2000) 1020–1029, http://dx.doi.org/10.1021/ie990758v.

[120] R. Fang, H. Huang, J. Ji, M. He, Q. Feng, Y. Zhan, D.Y.C. Leung, Efficient MnOx supported on coconut shell activated carbon for catalytic oxidation of indoor formaldehyde at room temperature, Chem. Eng. J. 334 (2018) 2050–2057, http://dx.doi.org/10.1016/j.cej.2017.11.176.

[121] J. Liu, S. Lu, L. Wang, T. Qi, D. Qi, X. Xing, Y. Zhang, H. Xiao, S. Zhang, Co-site substitution by Mn supported on biomass-derived active carbon for enhancing magnesia desulfurization, J. Hazard. Mater. 365 (2019) 531–537, http://dx.doi.org/10.1016/j.jhazmat.2018.11.040.

[122] C.F. Wu, M.A. Nahil, X. Sun, S. Singh, J.H. Chen, B.X. Shen, P.T. Williams, Novel application of biochar from biomass pyrolysis for low temperature selective catalytic reduction, J. Energy Inst. 85 (2012) 236–239, http://dx.doi.org/10.1179/1743967112Z.00000000033.

[123] M.J. Page, J.E. McKenzie, P.M. Bossuyt, I. Boutron, T.C. Hoffmann, C.D. Mulrow, L. Shamseer, J.M. Tetzlaff, E.A. Akl, S.E. Brennan, R. Chou, J. Glanville, J.M. Grimshaw, A. Hróbjartsson, M.M. Lalu, T. Li, E.W. Loder, E. Mayo-Wilson, S. McDonald, L.A. McGuinness, L.A. Stewart, J. Thomas, A.C. Tricco, V.A. Welch, P. Whiting, D. Moher, The PRISMA 2020 statement: An updated guideline for reporting systematic reviews, BMJ (2021) n71, http://dx.doi.org/10.1136/bmj.n71.

[124] S.M. Shaheen, Natasha, A. Mosa, A. El-Naggar, M.F. Hossain, H. Abdelrahman, N.K. Niazi, M. Shahid, T. Zhang, Y.F. Tsang, L. Trakal, S. Wang, J. Rinklebe, Manganese oxide-modified biochar: Production, characterization and applications for the removal of pollutants from aqueous environments - a review, Bioresour. Technol. 346 (2022) 126581, http://dx.doi.org/10.1016/j.biortech.2021.126581.

[125] M. Li, S. Kuang, Y. Kang, H. Ma, J. Dong, Z. Guo, Recent advances in application of iron–manganese oxide nanomaterials for removal of heavy metals in the aquatic environment, Sci. Total Environ. 819 (2022) 153157, http://dx.doi.org/10.1016/j.scitotenv.2022.153157.

[126] S.M. Husnain, U. Asim, A. Yaqub, F. Shahzad, N. Abbas, Recent trends of MnO_2-derived adsorbents for water treatment: A review, New J. Chem. 44 (2020) 6096–6120, http://dx.doi.org/10.1039/c9nj06392g.

[127] S. Wan, L. Qiu, Y. Li, J. Sun, B. Gao, F. He, W. Wan, Accelerated antimony and copper removal by manganese oxide embedded in biochar with enlarged pore structure, Chem. Eng. J. 402 (2020) http://dx.doi.org/10.1016/j.cej.2020.126021.

[128] S. Wan, L. Qiu, G. Tang, W. Chen, Y. Li, B. Gao, F. He, Ultrafast sequestration of cadmium and lead from water by manganese oxide supported on a macro-mesoporous biochar, Chem. Eng. J. 387 (2020) http://dx.doi.org/10.1016/j.cej.2020.124095.

[129] M.D. Chen, T. Wumaie, W.L. Li, H.H. Song, R.R. Song, Electrochemical performance of cotton stalk based activated carbon electrodes modified by MnO_2 for supercapacitor, Mater. Technol. 30 (2015) A2–A7, http://dx.doi.org/10.1179/1753555714Y.0000000241.

[130] S. Kong, B. Jin, X. Quan, G. Zhang, X. Guo, Q. Zhu, F. Yang, K. Cheng, G. Wang, D. Cao, MnO2 nanosheets decorated porous active carbon derived from wheat bran for high-performance asymmetric supercapacitor, J. Electroanal. Soc. 850 (2019) 567–577, http://dx.doi.org/10.1016/j.jelechem.2019.113412.

[131] S. Wang, B. Gao, Y. Li, Y. Wan, A.E. Creamer, Sorption of arsenate onto magnetic iron–manganese (Fe-Mn) biochar composites, RSC Adv. 5 (2015) 67971–67978, http://dx.doi.org/10.1039/c5ra12137j.

[132] P. Lodeiro, S. Kwan, J. Perez, L. González, C. Gérente, Y. Andrès, G. McKay, Novel Fe loaded activated carbons with tailored properties for as(V) removal: Adsorption study correlated with carbon surface chemistry, Chem. Eng. J. 215–216 (2013) 105–112, http://dx.doi.org/10.1016/j.cej.2012.11.052.

[133] L. Lin, W. Qiu, D. Wang, Q. Huang, Z. Song, H.W. Chau, Arsenic removal in aqueous solution by a novel Fe-Mn modified biochar composite: Characterization and mechanism, Ecotoxicol. Environ. Safety 144 (2017) 514–521, http://dx.doi.org/10.1016/j.ecoenv.2017.06.063.

[134] L. Lin, S. Zhou, Q. Huang, Y. Huang, W. Qiu, Z. Song, Capacity and mechanism of arsenic adsorption on red soil supplemented with ferromanganese oxide–biochar composites, Environ. Sci. Pollut. Res. 25 (2018) 20116–20124, http://dx.doi.org/10.1007/s11356-018-2188-7.

[135] L. Lin, G. Zhang, X. Liu, Z.H. Khan, W. Qiu, Z. Song, Synthesis and adsorption of Fe–Mn–La-impregnated biochar composite as an adsorbent for as(III) removal from aqueous solutions, Environ. Pollut. 247 (2019) 128–135, http://dx.doi.org/10.1016/j.envpol.2019.01.044.

[136] L. Lin, Z. Song, Y. Huang, Z.H. Khan, W. Qiu, Removal and oxidation of arsenic from aqueous solution by biochar impregnated with Fe-Mn oxides, Water Air Soil Pollut. 230 (2019) http://dx.doi.org/10.1007/s11270-019-4146-5.

[137] Z. Yu, L. Zhou, Y. Huang, Z. Song, W. Qiu, Effects of a manganese oxide-modified biochar composite on adsorption of arsenic in red soil, J. Environ. Manag. 163 (2015) 155–162, http://dx.doi.org/10.1016/j.jenvman.2015.08.020.

[138] P. Maneechakr, P. Chaturatphattha, S. Karnjanakom, Adsorption behavior of as(V) from aqueous solution by using Fe^{3+}–MnO_4–modified activated carbon (Leucaena leucocephala (Lam) de Wit), Res. Chem. Intermed. 44 (2018) 7135–7157, http://dx.doi.org/10.1007/s11164-018-3547-1.

[139] K.-W. Jung, S.Y. Lee, Y.J. Lee, Facile one-pot hydrothermal synthesis of cubic spinel-type manganese ferrite/biochar composites for environmental remediation of heavy metals from aqueous solutions, Bioresour. Technol. 261 (2018) 1–9, http://dx.doi.org/10.1016/j.biortech.2018.04.003.

[140] Z. Wu, X. Chen, B. Yuan, M.-L. Fu, A facile foaming-polymerization strategy to prepare 3D MnO2 modified biochar-based porous hydrogels for efficient removal of Cd(II) and Pb(II), Chemosphere 239 (2020) http://dx.doi.org/10.1016/j.chemosphere.2019.124745.

[141] D. Tiwari, S.M. Lee, Biomass-derived materials in the remediation of heavy-metal contaminated water: Removal of cadmium(II) and copper(II) from aqueous solutions, Water Environ. Res. 83 (2011) 874–881, http://dx.doi.org/10.2175/106143011X12928814445258.

[142] Z. Fan, Q. Zhang, M. Li, D. Niu, W. Sang, F. Verpoort, Investigating the sorption behavior of cadmium from aqueous solution by potassium permanganate-modified biochar: Quantify mechanism and evaluate the modification method, Environ. Sci. Pollut. Res. 25 (2018) 8330–8339, http://dx.doi.org/10.1007/s11356-017-1145-1.

[143] Y.-Y. Wang, H.-Y. Ji, H.-H. Lu, Y.-X. Liu, R.-Q. Yang, L.-L. He, S.-M. Yang, Simultaneous removal of Sb(III) and Cd(II) in water by adsorption onto a MnFe2O4-biochar nanocomposite, RSC Adv. 8 (2018) 3264–3273, http://dx.doi.org/10.1039/c7ra13151h.

[144] K.-W. Jung, S.Y. Lee, Y.J. Lee, Hydrothermal synthesis of hierarchically structured birnessite-type MnO2/biochar composites for the adsorptive removal of Cu(II) from aqueous media, Bioresour. Technol. 260 (2018) 204–212, http://dx.doi.org/10.1016/j.biortech.2018.03.125.

[145] B. Wang, F. Li, L. Wang, Enhanced hexavalent chromium (Cr(VI)) removal from aqueous solution by Fe–Mn oxide-modified cattail biochar: Adsorption characteristics and mechanism, Chem. Ecol. 36 (2020) 138–154, http://dx.doi.org/10.1080/02757540.2019.1699537.

[146] M. Liang, S. Xu, Y. Zhu, X. Chen, Z. Deng, L. Yan, H. He, Preparation and characterization of fe-mn binary oxide/mulberry stem biochar composite adsorbent and adsorption of cr(Vi) from aqueous solution, Int. J. Environ. Res. Public Health 17 (2020) http://dx.doi.org/10.3390/ijerph17030676.

[147] J.S. Fischel, M.H. Fischel, D.L. Sparks, Advances in understanding reactivity of manganese oxides with arsenic and chromium in environmental systems, in: ACS Symposium Series, American Chemical Society, 2015, pp. 1–27, http://dx.doi.org/10.1021/bk-2015-1197.ch001.

[148] M.J. Scott, J.J. Morgan, Reactions at oxide surfaces. 1. Oxidation of as(III) by synthetic birnessite, Environ. Sci. Technol. 29 (1995) 1898–1905, http://dx.doi.org/10.1021/es00008a006.

[149] C. Tournassat, L. Charlet, D. Bosbach, A. Manceau, Arsenic(III) oxidation by birnessite and precipitation of manganese(II) arsenate, Environ. Sci. Technol. 36 (2002) 493–500, http://dx.doi.org/10.1021/es0109500.

[150] L. Lin, M. Gao, X. Liu, Z. Song, Influence of the application of Fe-Mn-La ternary oxide-biochar composites on the properties of arsenic-polluted paddy soil, Environ. Sci.: Process. Impacts 22 (2020) 1045–1056, http://dx.doi.org/10.1039/c9em00570f.